Design, development and fabrication of PC based Quartz Crystal Microbalance and its implementation to study molecular recognition processes in lipid films

THESIS SUBMITTED TO

THE UNIVERSITY OF PUNE

FOR THE DEGREE OF

DOCTOR OF PHILOSOPHY

IN

INSTRUMENTATION SCIENCE

BY

NEELIMA SHANKARNARAYANAN IYER

Under the Guidance of

Dr. S. R. Gowariker
(Research Guide)

Dr. Murali Sastry
(Research Co-Guide)

PHYSICAL CHEMISTRY DIVISION
NATIONAL CHEMICAL LABORATORY
PUNE 411008
INDIA

NOVEMBER 2007

Dedicated to
My Daughter
Gayatri

CERTIFICATE

This is to certify that the work discussed in the thesis entitled “Design, development and fabrication of PC based Quartz Crystal Microbalance and its implementation to study molecular recognition processes in lipid films” by **Mrs. Neelima Shankarnarayanan Iyer**, for the degree of Doctor of Philosophy was carried out under my supervision. As per my guidance and suggestions the work was carried out at the Physical Chemistry Division, National Chemical Laboratory, Pune. Such materials, as has been obtained by other sources, have been duly acknowledged in this thesis. To the best of my knowledge, the present work or any part there of, has not been submitted to any other University for the award of any other degree or diploma.

Date: Dr. S. R. Gowariker

(Research Guide)

Place:

CERTIFICATE

This is to certify that the work discussed in the thesis entitled "Design, development and fabrication of PC based Quartz Crystal Microbalance and its implementation to study molecular recognition processes in lipid films" by **Mrs. Neelima Shankarnarayanan Iyer**, for the degree of Doctor of Philosophy was carried out under my supervision at the Physical Chemistry Division, National Chemical Laboratory, Pune. Such materials, as has been obtained by other sources, have been duly acknowledged in this thesis. To the best of my knowledge, the present work or any part there of, has not been submitted to any other University for the award of any other degree or diploma.

Date: Dr. Murali Sastry

(Research Co-guide)

Place:

DECLARATION

I, **Neelima Shankarnarayanan Iyer,** hereby declare that the work incorporated in this thesis entitled "Design, development and fabrication of PC based Quartz Crystal Microbalance and its implementation to study molecular recognition processes in lipid films" carried out by me at Physical Chemistry Division, National Chemical Laboratory, Pune, has not been submitted for the award of any other degree or diploma.

Date: **(Neelima Shankarnarayanan Iyer)**

Place:

Acknowledgement

I extend my sincere gratitude and appreciation to many people who made the Ph.D. thesis possible. First and foremost, I would like to extend my sincere thanks to my research guide Dr. S.R. Gowariker, Director, Tolani Education foundation, Pune and Former Director, Central Scientific Instrument Organisation, Chandigarh for his valuable guidance, inspiration and encouragement during the course of my research work. His constant support at each and every stage of the research work was invaluable. I consider myself to be very fortunate to get his guidance for the research work.

I express my deep sense of gratitude and sincere thanks to my research co-guide, Dr. Murali Sastry for his inspiring guidance and critical & valuable suggestions during experimentation. His constant support for Instrumentation applications has always been a source of inspiration for me.

I am extremely thankful to Mrs. Bhagyashree Joshi, Senior Research Fellow, Instrumentation & Communication Group, Physical Chemistry Division for her constant support, help and contribution in valuable technical discussions throughout my research work. I owe my sincere thanks to Mrs. Rupali Waichal, Technical Assistant, Instrumentation & Communication Group who has always helped in one way or the other during my research work.

I express my sincere thanks to Dr. S. Sivaram, Director, National Chemical Laboratory, and Dr. Sourav Pal, Head, Physical Chemistry Division for giving me the opportunity for this research work and making all the facilities available for the work.

I am extremely thankful to Dr. B.D. Kulkarni, Deputy Director & Head, Chemical Engineering and Process Development Division and The Chairman, In House projects Committee for providing the funds for ARM hardware and development tools.

I am thankful to Mr. A.M. Patil, Mr. M.S. Rajopadhye and Mr. B.D. Pazare, Engineering Services Unit for their kind help in the fabrication of flow cell as per the designed parameters.

I am thankful to Mr. Anand Bhave for his kind help and advice during the initial phase of research work.

I am grateful to Mr. Prashant Marathe, Oasis Technologies Pvt. Ltd., Pune for providing the ARM core for the compact development of QCM controller module.

I take this opportunity to thank my colleagues Mr. P.B. Kokney. Mr.S.S. Yerande, Mr. Mandar Kulkarni and my students Ms Kanchan Kulkarni, Ms Nazhat Shaikh, Mr. Rajeev Bansode who helped me at every point of the work whenever required.

I take this opportunity to thank research students from Nanoscience Group, Hrushikesh, Tanushree and Deepti who have helped me in all possible ways.

I feel deep sense of gratitude for my mother and father for their constant support & encouragement and for being tolerant towards my erratic hours of work. My sincere thanks to my elder brother Rajeev for his valuable support. My special thanks to Mr. Shankarnarayanan Iyer who always had a dream that I should complete Ph.D. work. My special thanks to my daughter Gayatri who has been the inspiration for me at every stage in my life and was extremely patient and tolerant towards my erratic hours of work As always, it is impossible to mention everybody who had an impact on my work. However, I take this opportunity to thank all my family members and friends for their blessings and well wishes throughout my life.

Abstract

The thesis discusses the indigenous design, development and fabrication of the Quartz Crystal Microbalance (QCM) and its implementation to study molecular recognition processes in lipid films. The developed instrument allows the user to perform the real-time measurement and plotting of frequency with auto scale facility. The developed instrument is compact, economical and can be used for in-situ measurements.

Chapter 1 is an Introduction chapter to the thesis and gives a brief overview about the interest in developing the system. The chapter describes the importance of QCM as a piezoelectric device capable of extremely sensitive mass measurement with several nanogram sensitivity. This chapter also discusses the standard QCM controllers which may not be useful for studying solution based in situ measurements. Chapter 2 discusses about the theory behind Quartz Crystal Microbalance. Basics of Quartz Crystals and selection of the same for in situ QCM is detailed. It also describes the importance of the Sauerbrey equation for mass calculations for monolayers formed at air-water interface. This chapter also talks about Langmuir films, the Langmuir-Blodgett (LB) technique and the instrumentation associated with this technique for depositing monolayers on Quartz crystals. Chapter 3 focuses on design, development and fabrication of Quartz Crystal Microbalance. The design of a QCM flow cell for in situ measurements has been discussed. Design and development of intelligent QCM controller has been discussed in detail. Selection of 80C320 microcontroller as the first step towards the micro hardware and interface development has been detailed. Finally, ARM RISC hardware has been incorporated, which has been explained as a System On Chip solution. Chapter 5 discusses about development of real time system software. A real time system software for frequency measurement of QCM crystal has been developed. Initially, assembly language software development has been done for 80C320 microcontroller and then ARM based software development has been done using "C" language and allied macros. This chapter also describes about the "C" based software development on PC side for uploading frequency data through serial RS232 bus from microcontroller and its real time plotting with auto scale facility. Chapter 5 is about experimental results and analysis. It describes about the basic experimentation carried out for developed QCM

was done by using standard surfactants to form the Langmuir monolayer. Their Pressure area isotherms were viewed for proper monolayer deposition and real time frequency measurements were recorded. The developed instrument was used to study a kinetic measurement of Octadecylamine (ODA) monolayer on different sub phases such as chloroplatenic acid (H_2PtCl_6), chloroauric acid ($HAuCl_4$) and hexafluorotitanate (K_2TiF_6). In-situ measurements were carried out for time dependent complexation of sodium borohydride ($NaBH_4$) - reduced gold nanoparticles on octadecylamine Langmuir monolayers. Chapter 6 is the Conclusions chapter and summarizes the work presented in the thesis. It gives the emphasis on the importance of QCM technique for studying complexation processes on nanoscale and for solution based studies of biological processes occurring on surfaces, particularly lipid films. This chapter describes the specifications of the developed system and it also discuses the scope of research for future developments in this area.

Table of Content

List of Figures

List of Tables

CHAPTER 1

INTRODUCTION

This chapter is an introduction to the thesis and gives a brief idea about the importance of the Quartz Crystal Microbalance. It presents the background of the thesis and discusses the objectives that have been taken during this research work. Finally, an outline of the thesis is given.

1.1 Introduction

The Quartz Crystal Microbalance (QCM) has been used in vacuum physics for many years for reliable thickness monitoring for metal film deposition. Recently, this technique has been refined to use in the liquid media. This way it is proving to be a sensitive means of monitoring interfacial processes quantitatively. Relevant to the surfactant science, the QCM has been used to study adsorption at the solid-liquid interface, wetting and spreading phenomena, detergency and interfacial surfactant electrochemistry [1-5]

The QCM earns its name from its ability to measure the mass of thin films that have adhered to its surface. The QCM unit operates when piezo-electric crystal wafer is caused to oscillate at a characteristic resonant frequency (F_0) by applying an alternate electric field across the electrodes. In 1880, Jacques and Pieree Curie discovered that mechanical stress applied to the surfaces of various crystals such as quartz, rochelle and tourmaline afforded a corresponding electrical potential across the crystal whose magnitude was proportional to the applied stress [11]. This behavior is referred to as the piezoelectric effect. The word piezoelectric derives from the word piezein, meaning to press. The frequency of a quartz crystal unit is limited by the physical dimensions of the vibrating quartz element. In AT cut crystals, the limiting dimension is the thickness of the vibrating quartz element. As the thickness is diminished, the frequency is increased. At some point usually around 30 MHz, the thickness of the quartz plate become too thin for manufacture processing. Usually for QCM experimentation, fundamental crystal units are used

1.2 Background and Purpose

In 1959, Sauerbrey published a paper that showed that frequency the shift of a quartz crystal resonator is directly proportional to the added mass on the electrodes. [12]. Sauerbrey's work is generally taken as the breakthrough and the first step towards a new quantitative tool to measure very small masses. Thus we can describe QCM to be an ultra-sensitive mass sensor.

When a uniform layer of foreign material is added to the surface of the quartz crystal, the acoustic wave will travel across the interface and will propagate through the layer. This leads to decrease in the frequency of the crystal. The frequency changes on deposition of the film can be converted to mass loading by using the Saurbrey formula [12].

$$\Delta f = -2 f_o^2 \times \frac{\Delta m}{A \times (\mu \times \rho)^{1/2}}$$

where Δf - frequency change, f_o - frequency of the crystal prior to a mass change, Δm - mass change, A - Piezo electrically active area, μ - shear modulus for quartz, ρ - density of quartz ($\mu = 2.95 \times 10^{11}$ g cm^{-1} s^{-2}, $\rho = 2.65$ g/cm^3).

There are situations where the Sauerbrey equation does not hold, when the added mass is,

not rigidly deposited on the electrode surface (s)

slips on the surface or

not deposited evenly on the electrode (s).

Therefore, Sauerbrey equation is strictly applicable to uniform, rigid thin film deposits. Due to this for many years QCM was regarded as a gas-phase mass detector. In the beginning of 1980s scientists realised that a quartz crystal can be excited to a stable oscillator when it was completely immersed in a liquid.

Quartz crystal based microbalance is a powerful tool to study various adsorption processes and has been extensively used to investigate adsorption of self-assembled monolayers (SAMs)[6], quality control of multilayers prepared by Langmuir-Blodgett films [7], nanoparticles [7,8], and biomolecules [9]. Jin et al. studied high activity enzyme microcrystal multilayer films constructed by layer-by-layer deposition of the polyelectrolyte coated catalase crystals and oppositely charged polyelectrolyte on QCM electrodes [10].

The developed QCM is a sensitive QCM for solution based studies of biological processes occurring on surfaces, particularly lipid films.

1.3 Objectives

To complete the QCM development following objectives were taken into consideration.

- Design and development of microcontroller based frequency controller

- Design and development of oscillator circuit for piezo electric crystal

- Design and fabrication of flow cell for QCM study in liquid medium.

- Design and development of serial coupling of frequency controller to personal computer to upload the frequency data in real time.

- Development of PC based software to read the real time frequency value and the plotting of the same with auto scaling facility.

- Design and fabrication of compact QCM controller module.

1.4 Overseas market study

Quartz crystal Microbalance instruments are available in the international market mainly from MAXTEK Inc. and KSV Instruments, Finland. The following models are available from these international companies.

1. **RQCM** : This is the research quartz crystal microbalance instrument developed by MAXTEK Incorporation, USA. It provides information of changes in mass of deposited layers on a quartz crystal. The mass change is proportional to the change in resonance frequency The instrument uses AT cut, 5, 6 and 9 MHz crystal for use in liquid medium.. The instrument is not equipped with display to read the real time frequency data. QCM is to be connected to PC using either RS232 interface or IEEE 488 interface to get the real time frequency value.

2. **KSV-QCMZ500**: This is the research quartz crystal microbalance instrument developed by KSV Instruments Ltd., Finland It provides information of changes in mass and viscoelastic properties of adsorped or deposited layers on a quartz crystal. The mass change is proportional to the change in resonance frequency and any viscoelastic behavior is revealed the change in electrical resistance. It uses AT cut, 5 MHz crystal for use in liquid medium. No display is attached with the instrument for reading the real time frequency value. The computer interface is RJ-45 ethernet

for frequency reading, display and data processing. The frequency resolution of KSV-QCMZ500 is 1 Hz.

All above mentioned models are available in the international market. The cost of above the instruments is more than Rs. 3,00,000.

While designing the instrument a detailed study has been done and all the designing criteria have been taken into consideration. The developed instrument is an indigenous development and is very compact. It has comparable resolution with commercially available instruments. Real time software has been developed to measure quartz crystal frequency and uploading the frequency value to PC for real time plotting and its file storage. Details specifications of the instrument are discussed in Chapter 6.

1.5 Highlights of subsequent chapters

Outline of the thesis is as follows.

Chapter 2: Theory – Quartz Crystal Microbalance

This chapter discusses the basics of Quartz Crystals and selection of the same for in situ QCM. It also describes the importance of the Sauerbrey equation for mass calculations for monolayers formed at air-water interface. This chapter also talks about Langmuir films, the Langmuir-Blodgett (LB) technique and the instrumentation associated with this technique for depositing monolayers on Quartz crystals.

Chapter 3: Design, development and fabrication of Quartz Crystal Microbalance

This chapter focuses on the indigenous development of the instrument that has been carried out during this research work. The design of a QCM flow cell for in situ measurements has been discussed. Design and development of intelligent QCM controller has been discussed in detail. Selection of 80C320 microcontroller as the first step towards the micro hardware and interface development has been detailed. Finally, ARM RISC hardware has been incorporated, which has been explained as a System on chip solution. The intelligent QCM controller is connected to a PC through a serial RS232 bus for real time data acquisition. The developed instrument is controlled through real time system software which is explained in Chapter 4.

Chapter 4: Development of real time system software

A real time system software for the frequency measurement of QCM crystal has been developed. Initially, assembly language software development has been done for 80C320 microcontroller and then ARM based software development has been done using "C" language and allied macros. This chapter also describes about the "C" based software development on PC side for frequency data collection through RS232 bus from micro and its real time plotting with auto scale facility.

Chapter 5: Experimental results and analysis:

The basic experimentation for developed QCM was done by using standard surfactants to form the Langmuir monolayer. Their Pressure area isotherms were viewed for proper monolayer deposition and real time frequency measurements were recorded. The results were found to be satisfactory and reproducible.

The following systems were studied using the developed instrument.

A Kinetic measurement of Octadecylamine (ODA) monolayer on different subphases

1. ODA on chloroplatenic acid (H_2PtCl_6)
2. ODA on chloroauric acid ($HAuCl_4$)
3. ODA on hexafluorotitanate (K_2TiF_6)

B: Time dependent complexation of sodium borohydride ($NaBH_4$) - reduced gold nanoparticles on octadecylamine Langmuir monolayers for in-situ measurements

Chapter 6: Conclusions

This chapter summarizes the work presented in the thesis. It gives the emphasis on the importance of QCM technique for studying complexation processes on nanoscale and for solution based studies of biological processes occurring on surfaces, particularly lipid films. This chapter also describes the specifications of the developed system and it also discuses the scope of research for future developments in this area.

References

[1] Z Lin, RM Hill, HT Davis, MD Ward, Langmuir 10:4060, 1994.

[2] Z Lin, T Stoebe, RM Hill, HT Davis, MD Ward, Langmuir 12:345, 1996.

[3] Z Lin, MD Ward, Anal Chem 68:1285, 1996.

[4] F Caruso, HA Rinia, DN Furlong, Langmuir 12:2145, 1996.

[5] A Weerawardena, CJ Drummond, F Caruso, M McCormick, Langmuir 14:575, 1998.

[6] (a) Wang, J.; Frostman, L. M.; Ward, M. D. J. Phys. Chem. 1992, 96, 5224-5228. (b) Buttry, D. A.; Ward, M. D. Chem. Rev. 1992, 92, 1355-1379. (c) Geddes, N. J.; Urquhart, R. S.; Furlong, D. N.; Lawrence, C.R.; Tanaka, K.; Okahata, Y. J. Phys. Chem. 1993, 97, 13767-13772.

[7] (a) Brust, M.; Etchonique, R.; Calvo, E.J.; Gordillo, G. J. Chem. Commun. 1996, 1949-1950. (b) Patil, V.; Mayya, K. S.; Pradhan, S. D.; Sastry, M. J. Am. Chem. Soc. 1997, 119, 9281-9282.

[8] (a) Bright, R. M.; Musick, M. D.; Natan, M. J. Langmuir 1998, 14, 5695-5701. (b) Sastry, M.; Patil, V.; Sainkar, S. R. J. Phys. Chem. B 1998, 102, 1404-1410. (c) Gole, A.; Sainkar, S. R.; Sastry, M. Chem. Mater. 2000, 12, 1234-1239.

[9] (a) Caruso, F.; Niikura, K.; Furlong, D. N.; Okahata, Y. Langmuir 1997, 13, 3427-3433. (b) Caruso, F.; Rodda, E.; Furlong, N. D.; Niikura, K.; Okahata, Y. Anal. Chem. 1997, 69, 2043-2049. (c) Gole, A.; Dash, C.; Mandale, A. B.; Rao, M.; Sastry, M. Anal. Chem. 2000, 72, 4301-4309. (d) Gole, A.; Chaudhari, P.; Kaur, J.; Sastry, M. Langmuir 2001, 17, 5646-5656.

[10] Jin, W.; Shi, X.; Caruso, F. J. Am. Chem. Soc. 2001, 123, 8121-8122.

[11] Curie, P.; Curie, J. C. R. Acad. Sci. 1880, 91, 294.

[12] Sauerbrey, G. Z. Phys. (Munich) 1959, 155, 206-222.

[13] Operation and service manual of RQCM by MAXTEK INC. USA

CHAPTER 2

THEORY – QUARTZ CRYSTAL MICROBALANCE

This chapter covers the basics of the Quartz crystal and principle of quartz crystal microbalance.

2.1 Basics of Quartz crystal

In 1880, Jacques and Pieree Curie discovered that mechanical stress applied to the surfaces of various crystals such as quartz, rochelle and tourmaline afforded a corresponding electrical potential across the crystal whose magnitude was proportional to the applied stress [6]. This behavior is referred to as the *piezoelectric effect*. This property exists only in materials that are acentric that is those which crystallize in noncentrosymmetric space groups. A single crystal of an acentric material will possess a polar axis due to dipoles associated with the orientation of atoms in the crystalline lattice. When stress is applied across an appropriate direction, there is a shift of dipoles resulting from the displacement of atoms. This atomic displacement leads to a corresponding change in the net dipole moment producing a net change in electrical charge on the faces of the crystal. (Figure. 2.1-I) The validity of the converse of this effect was also established wherein an application of a voltage across these crystals afforded a corresponding mechanical strain.

Detail study of piezoelectricity was started in 1917 when it was showed that quartz crystals can be used as transducers and receivers of ultrasound in water. In 1921 first quartz crystal controlled oscillator was described which was based on XT cut crystals, which have the drawback of being very temperature sensitive. This inverse piezoelectric effect is the basis of the quartz crystal microbalance (QCM) technique.

Application of electric field across the crystal causes a vibrational motion of the quartz crystal, with amplitude parallel to the surface of the crystal [1b]. The vibrational motion of the quartz crystal results in the establishment of transverse acoustic waves that propagates across the thickness of the crystal, reflecting back into the crystal at the surface. (Figure 2.1-I).

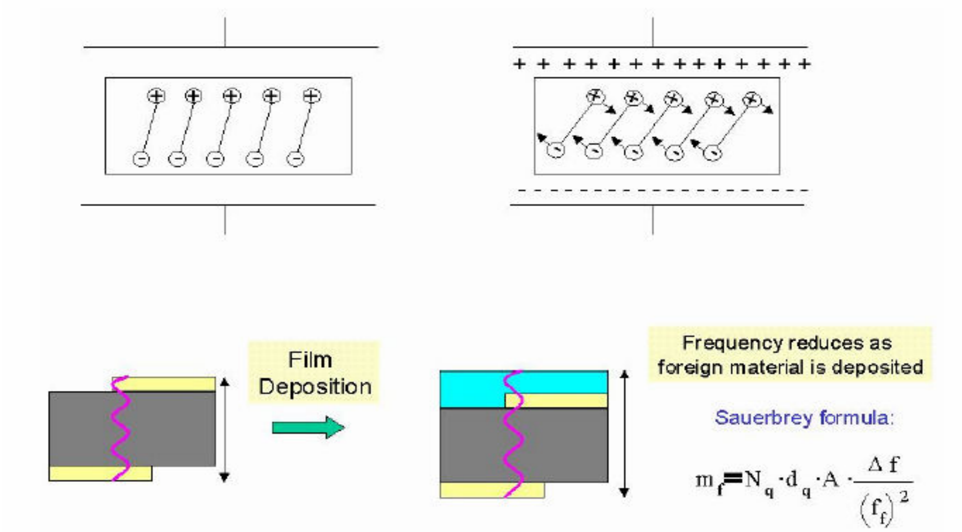

Figure 2.1 Schematic representation of the converse piezoelectric effect for shear motion. The electric field induces reorientation of the dipoles of the acentric material, resulting in a lattice strain and shear deformation of the material. Direction of shear is dependent upon the applied potential while the extent of shear strain depends on the magnitude of the applied potential.

2.2 Why AT cut crystal

Although a 20 of the 32 crystal systems lack a center of inversion and can exhibit piezoelectricity, the most commonly used piezoelectric material is a crystalline quartz (SiO_2). The advantage of using quartz over other crystals is that it is a completely oxidized material and insoluble in water. It can also resist temperatures up to 579 ^{0}C still maintaining its piezoelectricity. Its abundance on Earth's surface is incredible and is uniquely suited in terms of mechanical, electrical and chemical properties, for the manufacture of frequency control devices. Crystals cut with the proper angles with respect to the crystalline axes exhibit shear displacements. Depending on the cut angle, a large number of different resonator types such as thickness-shear mode, plate and flexural resonators can be obtained from a mother crystal with eigen frequencies ranging from $5x10^2 – 3\ x10^8$ Hz.

Generally AT-cut quartz crystals are used for QCM purposes in which thin quartz wafer is prepared by slicing a quartz rod at an angle of 35.25^0 with respect to the X-axis of the crystal, resonates in the *thickness shear mode*. AT cut quartz crystals exhibit a high frequency stability of .f/f~ 10^{-8}, which makes them well suited for many electronic devices. Since AT-cut quartz crystals have a temperature coefficient that is almost zero between 0-50 ^{0}C, this particular cut is the most suitable one for QCM sensors.

Figure.2.2 shows a gold coated QCM crystal.

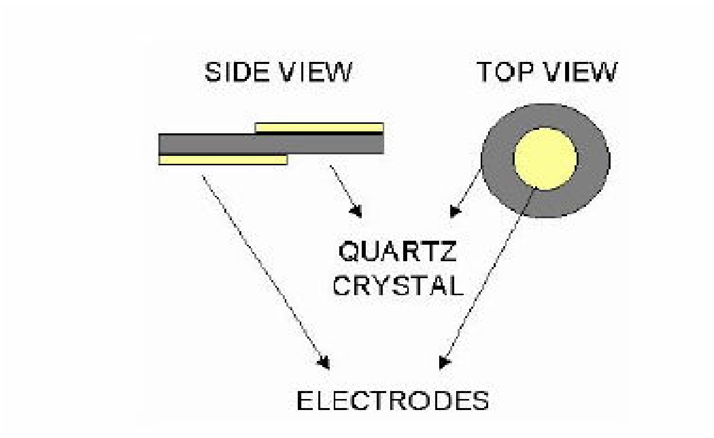

Figure 2.2 Diagram showing details of a quartz resonator

Although silver[9] and aluminium electrodes are used in surfactant studies, gold is used more often as gold surface provides more stable surface chemically. Silver and aluminium electrodes have tendency to oxidize in aqueous systems [9]. It has also been suggested that the thin gold electrodes of the QCM generally around 0.1 to 0.2 μm in thickness, may also be susceptible to incipient oxidation [10]. Solvents and sulphur containing compounds [11] such as "self –assembling alkane thiols" [12] can remove small amount of gold from the QCM surface.

The QCM unit operates when piezo-electric crystal wafer is caused to oscillate at a characteristic resonant frequency (F_0) by applying an alternate electric field across the electrodes. The frequency of a quartz crystal unit is limited by the physical dimensions of the vibrating quartz element. In AT cut crystals, the limiting dimension is the thickness of the vibrating quartz element. As the thickness is diminished, the frequency is increased. At some point usually around 30 MHz, the thickness of the quartz plate become too thin for manufacture processing. The crystal manufacturing processes differ for fundamental and overtone crystal units. Usually for QCM experimentation, fundamental crystal units are used. For the developed QCM, AT cut Quartz crystal with 9 MHz fundamental frequency is used. Current crystal manufacturing processes limit the lapping of the quartz plate so that the highest fundamental mode frequency that may be reliably achieved is typically around 45 MHz. At this frequency, the AT-cut quartz plate is less than 0.037 mm thick and further lapping using conventional techniques is not practical.

2.3 Frequency-Temperature Characteristics for AT-cut crystals

The frequency-temperature characteristic defines how the resonant frequency of the quartz crystal resonator varies in response to changes in temperature. For AT cut resonators, it is found that the frequency shift due to the variation of temperature can be expressed in a cubic curve of the form:

$$\Delta f/f_0 = a_0(T - T_0) + b_0(T - T_0)^2 + c_0(T - T_0)^3$$

T is the temperature variable and T_0 is the inflection temperature, which is approximately 25°C for the AT-cut. The coefficients a_0, b_0, and c_0 are the first, second, and third order temperature coefficients of frequency, and they are constants that depend on quartz properties and the angle of cut. The above equation gives a family of curves as shown below for four values of the relative cut angle. These curves show that a resonator can be designed to give a relatively small frequency variation over a broad temperature range.

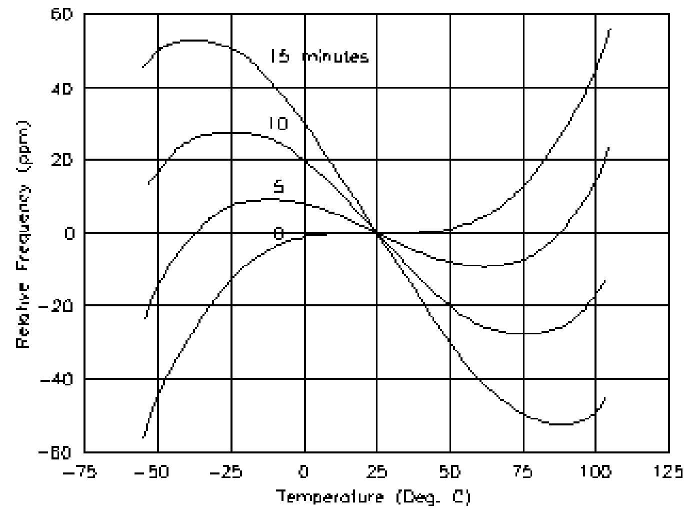

Figure 2.3 : AT-cut Frequency vs. Temperature Curves

Equivalent Circuit

A quartz crystal resonator is a mechanically vibrating system that is linked, via the piezoelectric effect, to the electrical world. It consists of a quartz plate with metal plating (electrodes), which is located on both sides of the quartz plate and is connected to insulated leads on the crystal package. Although the theoretical analysis of this device is a relatively complex electro-mechanical function, it can be expressed in terms of a simple equivalent circuit in the vicinity of the resonance frequencies as shown below:

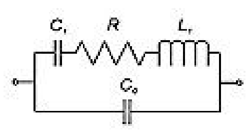

Equivalent electric circuit of quartz crystal resonator

The C_0, called the "shunt" or static capacitance, is the capacitance due to the electrodes on the crystal plate plus the stray capacitances due to the crystal enclosure. Shunt capacitance is present whether the crystal plate is oscillating or not (unrelated to the piezoelectric effect of the quartz). The R, C_1 and L_1 portion of the circuit is known as the "motional arm", which arises from the mechanical vibrations of the crystal. R represents the equivalent motional arm resistance; C_1 represents the motional capacitance of the quartz; and L_1 is the motional inductance, a function of the mass. The C_0 to C_1 ratio is a measure of the inter conversion between electrical and mechanical energy stored in the crystal, i.e., of the piezoelectric coupling factor, k. C_0/C_1 increases with the square of the overtone number. When a dc voltage is applied to the electrodes of a resonator, the capacitance ratio C_0/C_1 is also a measure of the ratio of electrical energy stored in the capacitor formed by the electrodes to the energy stored elastically in the crystal due to the lattice strains produced by the piezoelectric effect.

2.4 Sauerbrey Equation

In 1959, Sauerbrey showed that frequency shift of a quartz crystal resonator is directly proportional to the added mass on the electrodes. [7]. Sauerbrey's work is generally taken as the breakthrough and the first step towards a new quantitative tool to measure very small masses that are quartz crystal microbalance. Thus we can describe QCM to be an ultra-sensitive mass sensor.

When a uniform layer of foreign material is added to the surface of the quartz crystal, the acoustic wave will travel across the interface and will propagate through the layer. This leads to decrease in the frequency of the crystal. The details have been depicted in Figure.2.1. The frequency changes on deposition of the film can be converted to mass loading by using the Saurbrey formula [7].

$$\Delta f = -2 f_o^2 \times \frac{\Delta m}{A \times (\mu \times \rho)^{1/2}}$$

where Δf - frequency change, f_o - frequency of the crystal prior to a mass change, Δm - mass change, A - Piezo electrically active area, μ - shear modulus for quartz, ρ - density of quartz ($\mu = 2.95 \times 10^{11}$ g cm^{-1} s^{-2}, $\rho = 2.65$ g/cm^3).

There are situations where the Sauerbrey equation does not hold , when the added mass is

a. not rigidly deposited on the electrode surface (s)
b. slips on the surface
c. not deposited evenly on the electrode (s)

Therefore, Sauerbrey equation is strictly applicable to uniform, rigid thin film deposits. Due to this for many years QCM was regarded as a gas-phase mass detector. In the beginning of 1980s scientists realised that a quartz crystal can be excited to a stable oscillator when it was completely immersed in a liquid.

2.5 Selection of Quartz crystal unit

Following parameters have to be considered for selection of Quartz crystal unit

1. Frequency
2. Blank diameter
3. Surface finish
4. Electrode diameter
5. Electrode material
6. Mounting
7. Bonding

Blank Diameter

The standard Blank Diameters are .538", .340", and .318" for most common frequencies such as 9MHz and 10 MHz. Frequencies outside of the normal range may require different diameters.

Surface Finish

Quartz crystals with unpolished and polished surface finish are available.

1. Etched (un-polished), has less than a 3 micron finish. An etched surface finish increases the effective surface area of the electrode. No adhesion layer is required for etched surfaces unless it is to be operated in a harsh environment or at high temperatures. Etched surface finishes are used for electrochemical applications.
2. Polished (optically clear), has less than a 1 micron finish. A polished surface finish provides a more consistent surface area on the electrode. Polished surfaces require an adhesion layer underneath the primary metallization such as Chromium (Cr) or Titanium (Ti).

Electrode Diameter

Electrodes are normally .137", .201", or .268" in diameter depending on the frequency requested.

Electrode Material

Normally QCMs plated with 1,000 Å of 99.99% pure gold (Au) are supplied. Other electrode materials that are available include:

Aluminum (Al)	Molybdenum (Mo)	Silver (Ag)
Carbon (C)	Nickel (Ni)	Tin Oxide (SnO_2)
Chromium (Cr)	Palladium (Pd)	Titanium (Ti)
Cobalt (Co)	Platinum (Pt)	Tungsten (W)
Copper(Cu)	Silicon (Si)	Zinc (Zn)

Mounting and Bonding

QCM crystals are normally supplied mounted and bonded to an HC-48/U base which provides physical and electrical connection. Mounted and bonded crystals are easy to handle during experimentation.

QCM crystals used for developed QCM instrumentation are procured from International Crystal Manufacturing Company, USA. The specifications of crystal are as mentioned under.

Frequency: 9 MHz

Diameter: 1 inch

Surface finished : Polished

Electrode material : 100 A^0 Cr / 1000 A^0 Au

Blank diameter: 0.538 inch

Electrode diameter: 0.201 inch

Mounted and bonded to HC-48/U base (for easy handling during experimentation)

2.6 Langmuir films

Langmuir films [13] consist of surface active materials or *surfactants* trapped at the interface between two dissimilar phases, either liquid-liquid or liquid-gas. Surfactants are molecules, which are amphiphilic in nature (Figure 2.6-I) and consist of a hydrophilic (water soluble) and hydrophobic (water insoluble) part. The hydrophobic part usually consists of hydrocarbon or fluorocarbon chains and the forces acting upon them are predominantly van der Waal's force. The hydrophilic part consists of a polar group (-OH, -COOH, $-NH_3^+$, $-PO_4^-(CH_2)_2NH_3^+$ etc.) and the forces acting upon them are predominantly Coulomb forces.

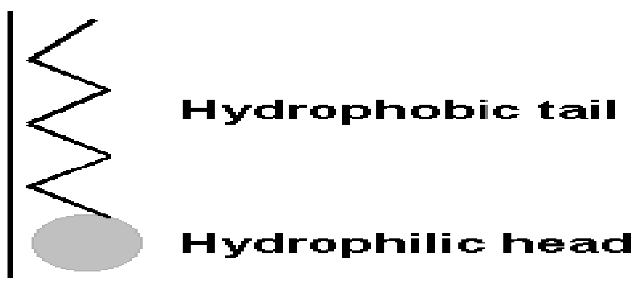

Figure 2.6-I Schematic of an amphiphilic molecule showing hydrophobic (long hydrocarbon chain) and hydrophilic (polar group) parts

Amphiphilic molecules are trapped at the interface because they possess two different types of bonding within the one molecular structure. The driving force behind the association is the reduction of the free energy of the system. Therefore, when a surfactant comes in contact with water, it accumulates at the air-water interface causing a decrease in the surface tension of water. Many of these amphiphilic molecules insoluble in water can (with the help of a volatile and water insoluble solvent) be easily spread on the water surface with hydrophilic *head* groups pulling the molecule into the bulk of the water and the hydrophobic *tail* groups pointing into the air. One molecule thick surface monolayer will only be achieved if the amphiphilic balance (balance between hydrophilic and hydrophobic parts) of the molecule is correct. Sweeping a barrier over the water surface causes the molecules to come closer together and eventually form a compressed and an ordered monolayer. The film produced by such a method is known as a Langmuir film [14]. The amphiphilic nature of the surfactants dictates the orientation of the molecules at the air-water interface in such a way that the polar head group is immersed in the water and the long hydrocarbon chain is pointing towards air (Figure 2.6-II).

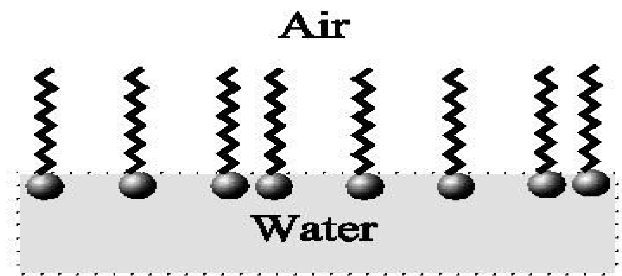

Figure 2.6-II A spread monolayer at the air-water interface

The hydrocarbon chain of the substance used for monolayer studies has to be long enough to form an insoluble monolayer. There should be minimum 12 hydrocarbons or groups in the chain. If the chain is shorter, though still insoluble in water, the amphiphile on the water surface tends to form micelles. These micelles are water soluble, which prevents the build-up of a monolayer at the interface. On the other hand, if the length of the chain is too long, the amphiphile tends to crystallize on the water surface and consequently does not form a monolayer. Furthermore, the amphiphile has to be soluble in some organic solvent that is highly volatile and water insoluble. Chloroform or hexane is commonly used for this purpose.

2.6.1 Surface pressure area isotherms

The most important indicator of the monolayer properties of an amphiphilic material is given by measuring the surface pressure as a function of the area of water surface available to each molecule. This is carried out at constant temperature and is known as a surface pressure area isotherm or simply *isotherm*.

When a solution of an amphiphile in a water insoluble solvent is placed on the water surface with a micro syringe, the solution spreads rapidly to cover the available area. As the solvent evaporates, a monolayer is formed. When the available area for the monolayer is large, the distance between adjacent molecules is large and their interactions are weak. Then, the monolayer can be regarded as a two-dimensional gas. Under these conditions, the monolayer has little effect on the surface tension of water. If the available surface area of the monolayer is reduced by a barrier system, the molecules start to exert a repulsive effect on each other. This two-dimensional analogue of pressure is called surface pressure [14], and is given by the following relationship

$$\pi = \gamma - \gamma_o$$

where, γ is the surface tension of pure water surface and γ_o is the surface tension with the monolayer.

Usually an isotherm is recorded by compressing the film (reducing the area with the barriers) at a constant rate while continuously monitoring the surface pressure. Depending on the material being studied, repeated compressions and expansions may be necessary to achieve a reproducible trace. Figure 2.6-III shows the typical pressure area isotherm and various phase transitions of the floating monolayer.

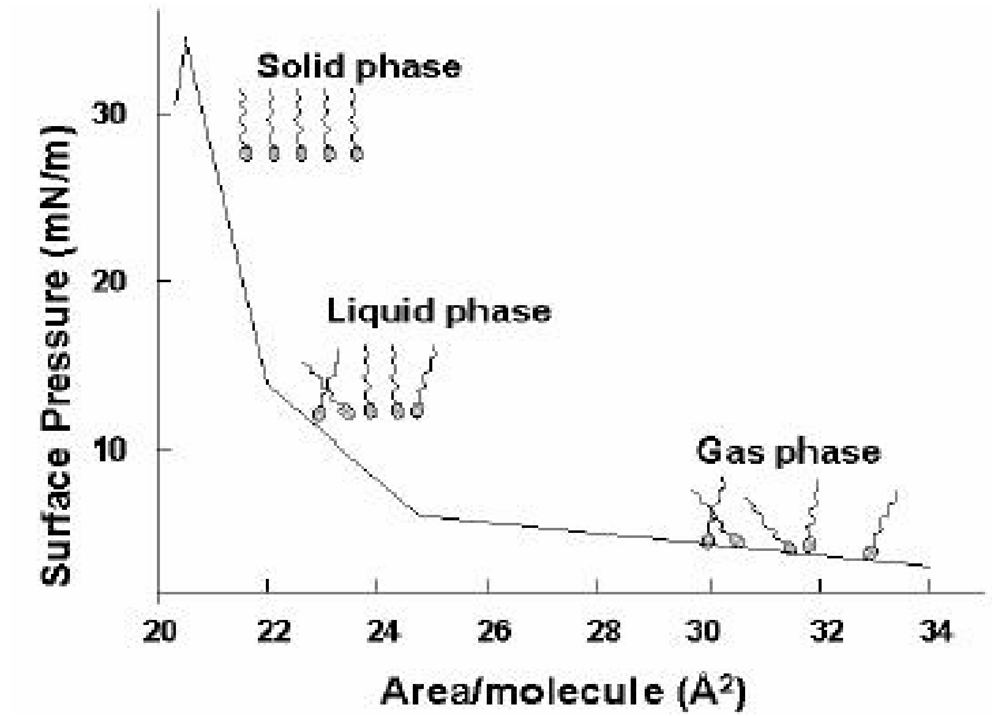

Figure 2.6-III Typical pressure area (π–A) isotherm showing the various phase transitions of the floating monolayer

As early as 1952, W. D. Harkins proposed a simple terminology to classify different monolayer phases of an amphiphile molecule [15]. Initially, the monolayer exists in the gaseous state (G) and on compression can undergo a phase transition to the liquid-expanded state (LE). Upon further compression, the LE phase undergoes a transition to the liquid-condensed state (LC), and at even higher densities, the monolayer finally reaches the solid state (S). If the monolayer is further compressed after reaching state S, the monolayer will collapse into three-dimensional structures. The collapse is generally seen as a rapid decrease in the surface pressure or as a horizontal break in the isotherm if the monolayer is in a liquid state. This collapse pressure is a function of the temperature, the pH of the sub phase and the speed by which the barrier is moved.

An isotherm gives the information about the stability of the molecules in the two-dimensional system, phase transitions and conformational transitions. It also gives some idea of the amount of pressure that has to be applied to the film on the sub phase to enable deposition of the LB film in the solid phase. Thus, at appropriate pressure, the film can be transferred to the substrate.

2.7 NIMA Langmuir – Blodgett (LB) trough model 611D

NIMA LB trough model 601S has been used for QCM experimentation. It consists of Barrier mechanism, Pressure sensor PS4, Dipper mechanism, interface to PC, Graphical User Interface software on PC for trough operation. An intelligent microcontroller 80C552 based controller unit takes care of controlling of opening and closing the barrier, pressure sensing and controlling the dipper mechanism. The microcontroller unit is coupled to PC through RS232 interface. GUI has a facility to choose either COM1 / COM2 serial interface for NIMA trough. Required parameters are set by user using GUI, which then are downloaded to microcontroller unit through RS232. During operation of the trough, the surface pressure of a monolayer is uploaded to PC through RS232. GUI takes care of plotting real time pressure area isotherm.

References

[1] (a) Wang, J.; Frostman, L. M.; Ward, M. D. *J. Phys. Chem.* **1992**, *96*, 5224-5228. (b) Buttry, D. A.; Ward, M. D. *Chem. Rev.* **1992**, *92*, 1355-1379. (c) Geddes, N. J.; Urquhart, R. S.; Furlong, D. N.; Lawrence, C.R.; Tanaka, K.; Okahata, Y. *J. Phys. Chem*. **1993**, *97*, 13767-13772.

[2] (a) Brust, M.; Etchonique, R.; Calvo, E.J.; Gordillo, G. J. *Chem. Commun.* **1996**, 1949-1950. (b) Patil, V.; Mayya, K. S.; Pradhan, S. D.; Sastry, M. *J. Am. Chem. Soc*. **1997**, *119*, 9281-9282.

[3] (a) Bright, R. M.; Musick, M. D.; Natan, M. J. *Langmuir* **1998**, *14*, 5695-5701. (b) Sastry, M.; Patil, V.; Sainkar, S. R. *J. Phys. Chem. B* **1998**, *102*, 1404-1410. (c) Gole, A.; Sainkar, S. R.; Sastry, M. *Chem. Mater*. **2000**, *12*, 1234-1239.

[4] (a) Caruso, F.; Niikura, K.; Furlong, D. N.; Okahata, Y. *Langmuir* **1997**, *13*, 3427-3433. (b) Caruso, F.; Rodda, E.; Furlong, N. D.; Niikura, K.; Okahata, Y. *Anal. Chem.* **1997**, *69*, 2043-2049. (c) Gole, A.; Dash, C.; Mandale, A. B.; Rao, M.; Sastry, M. *Anal. Chem.* **2000**, *72*, 4301-4309. (d) Gole, A.; Chaudhari, P.; Kaur, J.; Sastry, M. *Langmuir* **2001**, *17*, 5646-5656.

[5] Jin, W.; Shi, X.; Caruso, F. *J. Am. Chem. Soc.* **2001**, *123*, 8121-8122.

[6] Curie, P.; Curie, J. C. R. *Acad. Sci.* **1880**, *91*, 294.

[7] Sauerbrey, G. *Z. Phys. (Munich)* **1959**, *155*, 206-222.

[8] Wang, J.; Frostman, L.M.; Ward, M.D. *J. Phys. Chem.* **1992**, *96*, 5224. (b) Buttry, D. A.; Ward, M.D. *Chem. Rev.* **1992**, *92*, 1356.

[9] K Ijiro, M Shimomura, M Tanaka, H Nakamura, K Hasebe. Thin Solid Films 284-285:780, **1996**

[10] JJ Donohue, DA Buttry. Langmuir 5:671, **1989**

[11] NJ Geddes, EM Paschinger, DN Furlong, F Caruso, CL Hoffmann, JF Rabolt. Thin Solid Films 260:192, **1995**

[12] Y Xia, XM Zhao, GM Whitesides. Microelectronic Engineering 32:255, **1996**

[13]"Insoluble Monolayers at Liquid Gas Interface", G. L. Gaines Jr., *Interscience*, New York, 1966.

[14] "Langmuir and Langmuir Blodgett films: What and How?", Application note #107, KSV instruments Ltd., Finland.

[15] Ulman A., *An introduction to Ultrathin Organic Films: from Langmuir-Blodgett to Self-Assembly*, Academic Press, San Diego, CA, 1991.

[16] Technical manual from NIMA Technology, England.

CHAPTER 3

DESIGN, DEVELOPMENT AND FABRICATION OF QUARTZ CRYSTAL MICROBALANCE

This chapter focuses on the indigenous development of the instrument that has been carried out during this research work. The design of a QCM flow cell for in situ measurements has been discussed. Design and development of intelligent QCM controller has been discussed in detail.

This chapter focuses on the indigenous development of the instrument that has been carried out during this research work. The design of a QCM flow cell for in situ measurements has been discussed. Design and development of intelligent QCM controller has been discussed in detail. Selection of 80C320 microcontroller as the first step towards the micro hardware and interface development has been detailed. Finally, ARM RISC hardware has been incorporated, which has been explained as a System on chip solution. The intelligent QCM controller is connected to a PC through a serial RS232 bus for real time data acquisition. The developed instrument is controlled through real time system software which is the next chapter of the thesis.

3.1 Design objective

It was decided to design and developed QCM with microcontroller as an base intelligence with interface facility of serial RS232, USB and Ethernet for measured frequency storage and uploading to PC. Designed QCM does not measure the particular frequency and works for frequency measurement up to 10MHz. The flow cell is designed for in-situ measurements which would be helpful for Scientists and researchers for their research. The developed QCM is an indigenous development. The instrumentation uses up-to-date technology of System On Chip (SOC) solution using ARM microcontroller.

3.2 Description of QCM set-up

The developed QCM set up consists of different assemblies as described in the Section 3.3 onwards. A typical QCM set up is as shown in Figure. 3.1. An intelligent QCM controller was developed by using 80C320 microcontroller first and then to make the controller instrumentation more compact and to add innovative features, Phillips make LPC2148 ARM microcontroller hardware was developed. QCM controller is not designed for a particular frequency. It can measure the frequency up to 10 MHz. Flow cell was designed for in –situ measurements. The measure frequency of QCM crystal can be uploaded to PC using RS232 serial interface for real time plotting with auto scale facility. Figure 3.2 shows the set up for QCM measurements using 80C320 microcontroller hardware.

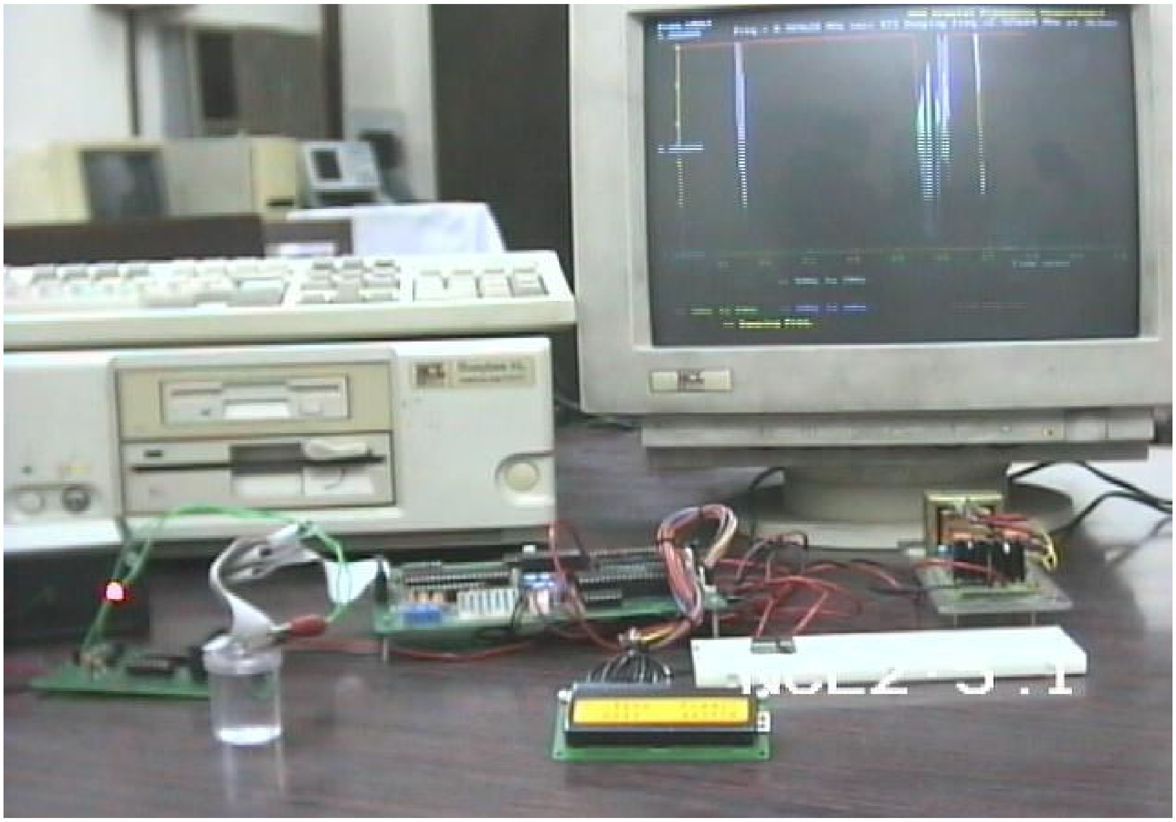

Figure 3.2: Developed Quartz Crystal Microbalance Set Up

3.3 Flow Cell Design

It was decided to design and develop flow cell for in-situ measurements for QCM experimentation. The material used for flow cell was acrylic to its transparency and inert chemical nature. Flow cell was designed to fit the QCM crystal between two plates of QCM flow cell for in-situ measurements. Please refer to Figure. 3.3-I and Figure 3.3-II.

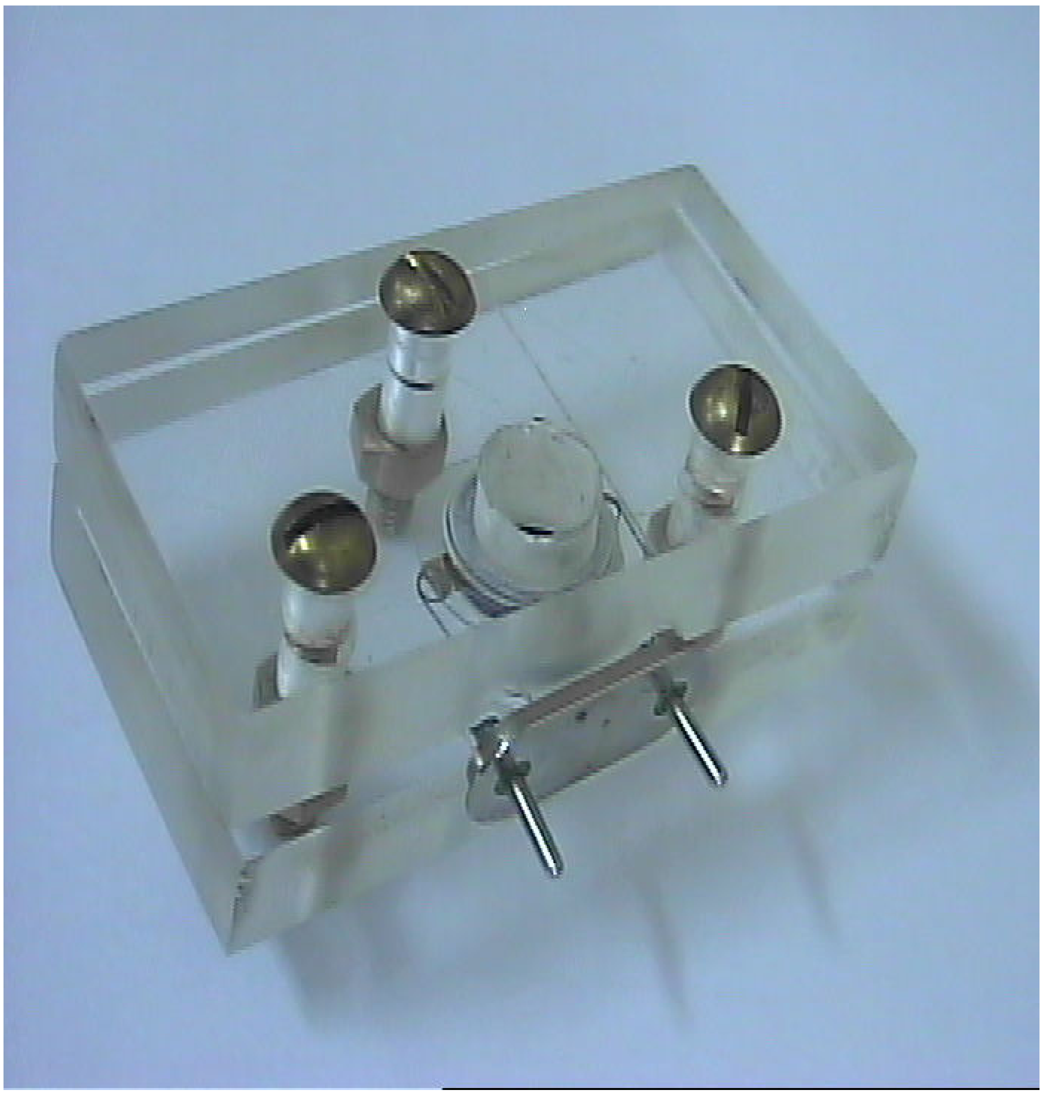

Figure 3.3-I: QCM flow cell- side view (with quartz crystal fitted)

Figure 3.3-II: QCM flow cell- top view (with quartz crystal fitted)

Mechanical drawing of the flow cell is attached as shown in Figure. 3.3-III.

Crystal was fitted between two Viton “O” rings so that the liquid put the in the flow cell for in-situ measurement should not spill off.

The technical details of Viton “O” rings are as follows:

Outer diameter:- 11 mm

Inner diameter - 8 mm.

Flow cell is designed for 100 µl capacity for in-situ measurement.

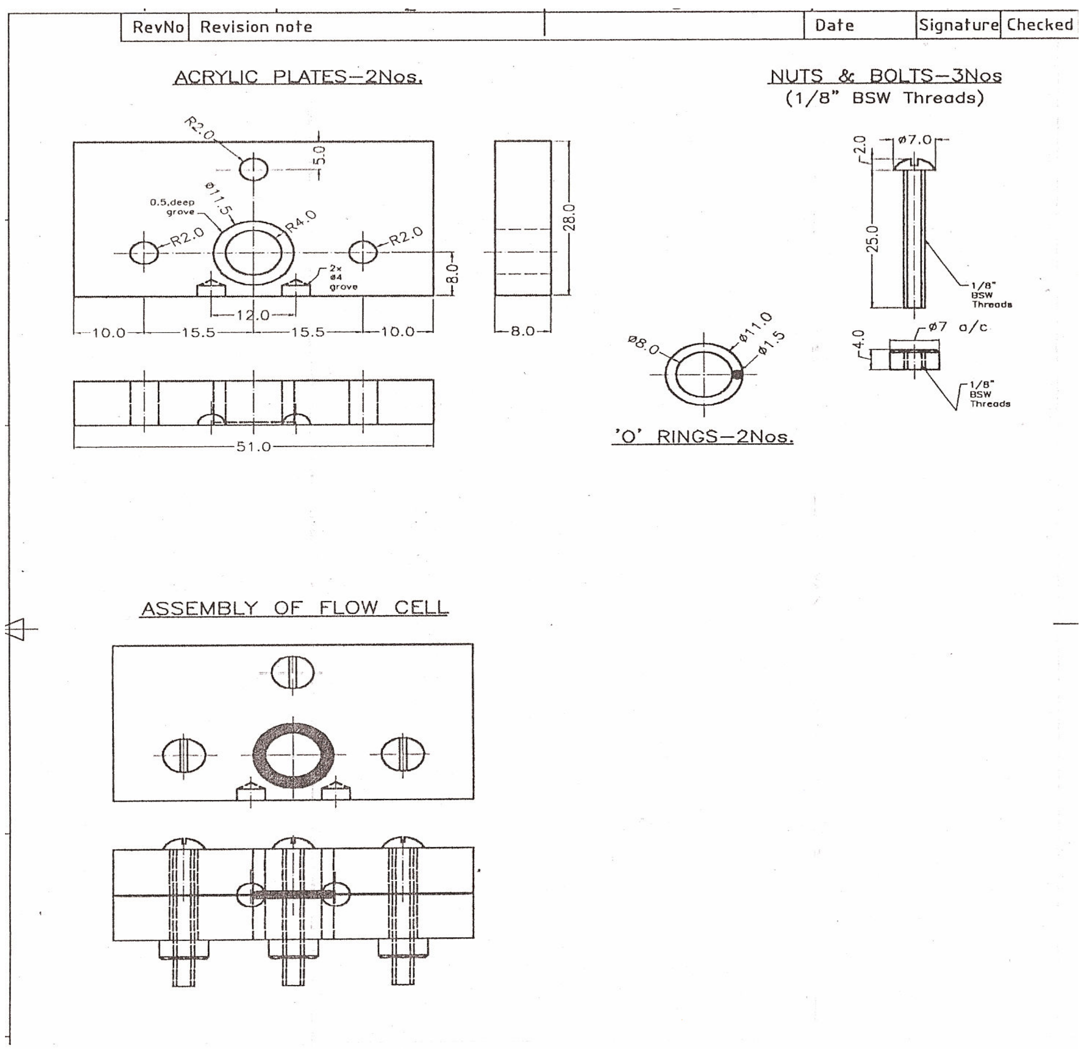

Fig. 3.3. III: Mechanical drawing of flow cell

3.4 QCM controller design

3.4.1. Choice of microcontroller

The need of microcontroller for QCM controller design is inevitable. The intelligence in form of microcontroller is responsible for real time frequency measurement and also communicating the frequency value to the PC using serially using RS232 protocols. For more than two decades, I had carried out the work for microprocessor / microcontroller based instrumentation using Z-80 processor, 8748 / 8749 microcontrollers, 8031 / 8751 / 89C51 microcontroller and higher derivatives of 51 series such as 80C552. The hand coding was done for Z-80 and 8748/49 based development and assembly language programming was done for 51 series microcontroller. Since the development tool like assembler and programmer was available for 51 series, it was decided to make use of suitable microcontroller from 51 series. As discussed in 3.4, QCM controller requires the I/O peripherals like keys, 16 x 2 LCD display, serial communication, RTC chip interface, counter interface, it is appropriate to use 8031 microcontroller with external peripherals like Flash EPROM, Programmable Peripheral Interface 8255, and RTC DS1237. Maximum operating frequency for 8031 micro is upto 12 MHz and hence it was decided to use speedy and available microcontroller 80C320 with operating frequency as 30 MHz. To make the QCM controller more compact, a further development was carried out using Phillips LPC2148 ARM controller.

3.4.2 80C320 based microcontroller hardware design

The microcontroller hardware platform is designed to accommodate required peripherals with minimum number of interface chips. Please refer to Figure. 3.4-I showing the peripherals connected to the microcontroller 80C320.

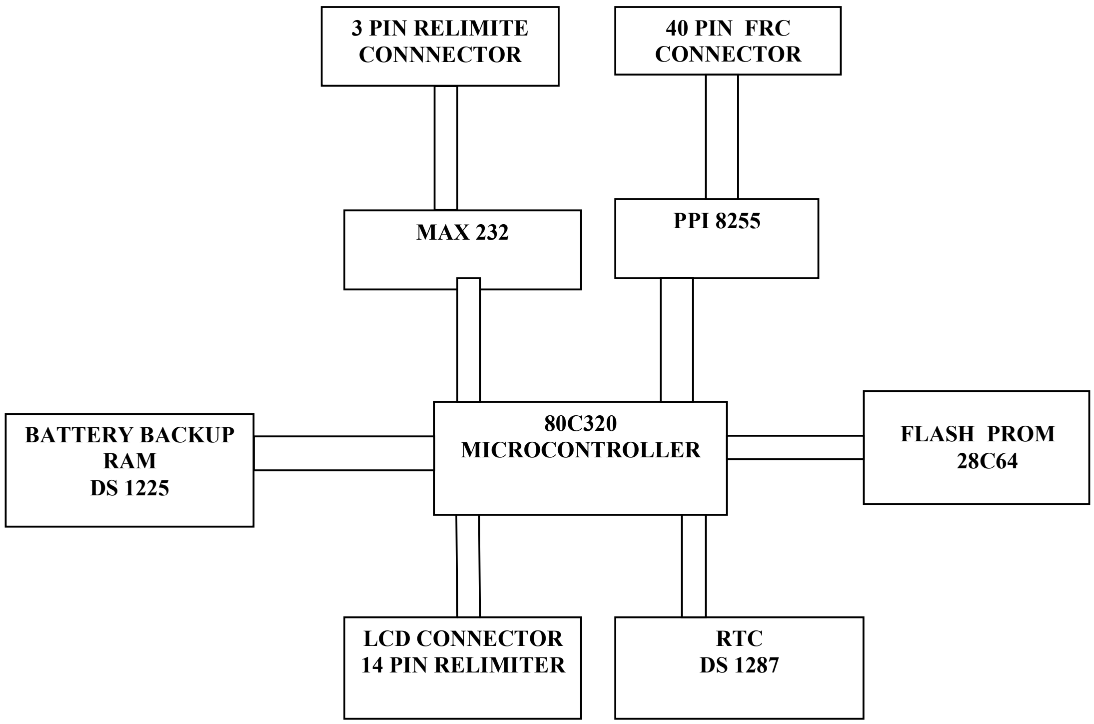

Figure 3.4-I Block diagram of 80C320 microcontroller hardware

The designed and developed hardware platform using 80C320 is shown in Figure. 3.4-II.

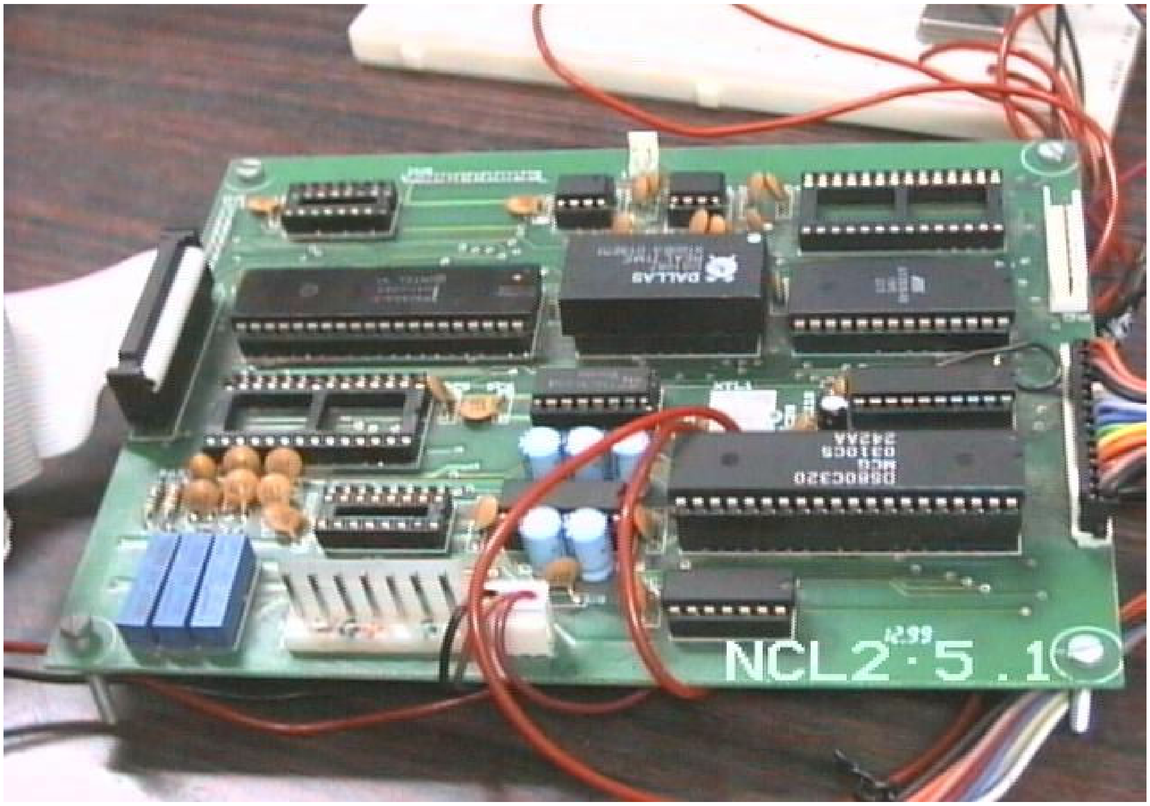

Figure 3.4-II -Developed board for 80C320 microcontroller hardware

The architecture feature of MCS51 family is input and output peripherals are memory mapped I/Os.

Memory map for 80C320 hardware is as follows:

Flash EPROM 28C64 : 0000H – 3FFFh

NVRAM DS1225 : 4000H – 7FFFH

PPI 8255 : 8000H-CFFFh

RTC DS1287 - extended RAM design

LCD is not memory mapped.

3.4.2.1 LCD Interface

LCD of two lines and 16 characters per line (16 x 2) is used to display the measured frequency. The LCD has microcontroller intelligence and provides 14 pin

LCD connector definition for its use to interface with microcontroller or microprocessor. Please refer to Figure.3.4-III. for LCD interface with 80C320 microcontroller.

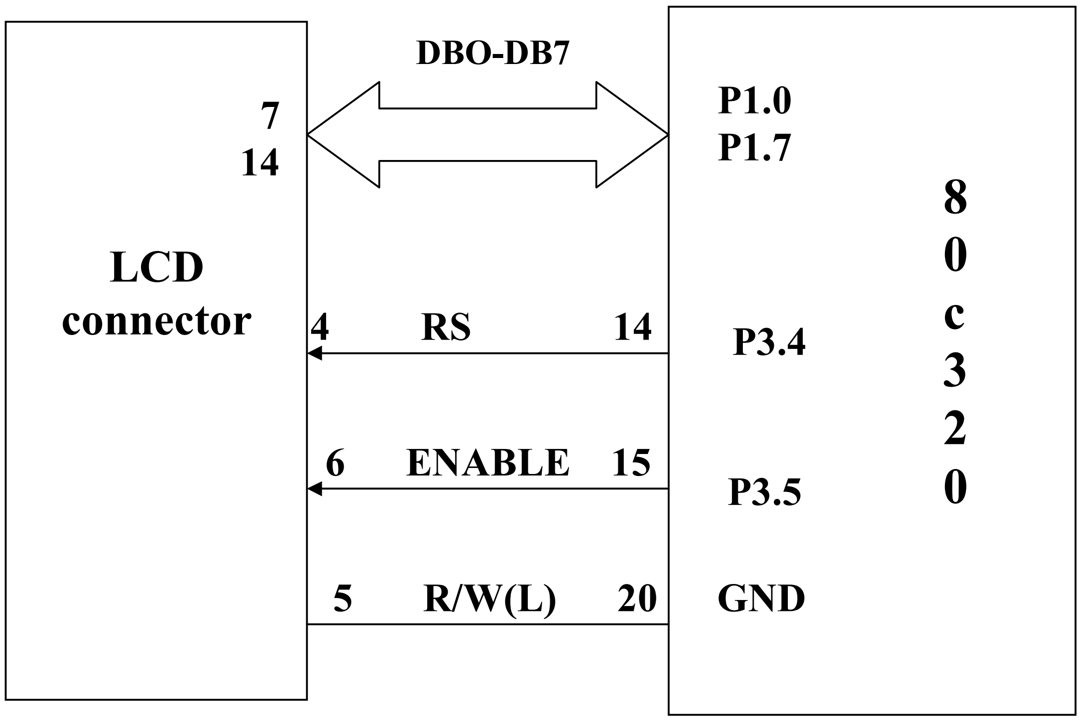

LCD connector- Pin1 – GND Pin 2 – Vcc
Pin 3- V intensity – GND for maximum intensity
R/W(L) means active low for W(write) and active high for R(read)

Figure 3.4-III LCD Interface

A chip select which is the Enable pin of LCD is connected to P3.5 port line of microcontroller. Thus LCD peripheral is not memory mapped peripheral for this 80C320 microcontroller. Once a particular character ASCII code is written to DDRAM of LCD, some millisecond time is taken by LCD for the display of same. During this time, BUSY flag is set which can be read by connecting read / write pin to the controller port pin and declaring that pin in input mode through program. Once the BUSY flag is reset, means next character can be written to DDRAM of LCD. For this operation, port pin connected to read / write pin of LCD has to be declared in output mode through program. Instead of waiting for the BUSY flag to get reset, the required amount of software delay is executed. So read / write pin functions only in write mode. The Write signal being active low, pin 5 of LCD connector is grounded and thus one port line of microcontroller is saved.

3.4.2.2 RTC Interface

RTC DS1287 interface with 80C320 microcontroller is shown in Figure. 3.4-IV

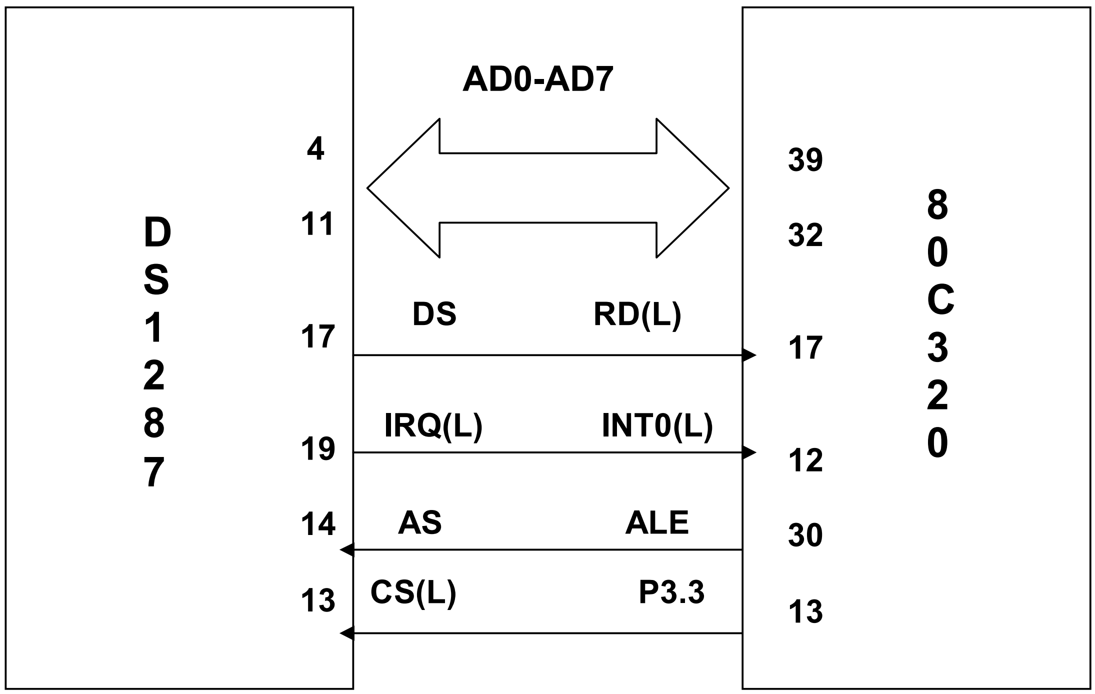

Figure 3.4-IV RTC Interface

RTC chip is designed in the extended RAM design mode. MCS51 family microcontrollers have facility to design and develop interface with peripherals like 8155 (RAM plus I/O) or 8355 (ROM plus I/O). RTC DS1287 has 40 bytes of on chip RAM and can be accessed by microcontroller using the instructions

MOVX A, @R0 OR MOVX @R0,A.

The chip select is connected to P3.3 port pin of microcontroller which is programmed as output pin. Thus RTC DS1287 is not memory mapped peripheral for this 80C320 based design for QCM controller.

3.4.2.3 Crystal Oscillator and Frequency counter interface

Sometimes an input signal to a digital circuit doesn't directly fit the description of a digital signal. For various reasons it may have slow rise and/or fall times, or may have acquired some noise that could be sensed by further circuitry. It may even be an analog signal whose frequency we want to measure. All of these conditions, and many others, require a specialized circuit that will force it to true digital shape. The required circuit to be used for this purpose is schmitt trigger. It has two possible states just like other multivibrators. However, the trigger for this circuit to change states is the input voltage level, rather than a digital pulse. That is, the output state depends on the input level, and will change only as the input crosses a pre-defined threshold. Quartz crystal oscillator is designed using Hex Inverter Schmitt Trigger IC 74HC14. Please refer to Figure. 3.4-V The 10K resistance and two 33pf tantalum capacitors are used for this design.

The QCM crystal oscillator output is connected to the counter input pin 10 of 12 bit binary counter IC CD4040. Please refer to Figure. 3.4-V. On negative going edge of clock pulse at pin 10, the counter gets incremented. A binary count is more than 16 bits for measuring the frequency of 10 MHz. One 12 bit binary counter count pulses up to 2^{12} bits (3 nibbles) and so one more 12 bit binary counter is cascaded to the first one. Two 12 bit binary counters give facility to measure up to 2^{24} bits (6 nibbles). The output status Q1 – Q12 of each counter is connected to the IC 8255 on 80C320 microcontroller board through 40 pin Flat Ribbon Cable (FRC) connector. Please refer to Table 3.1

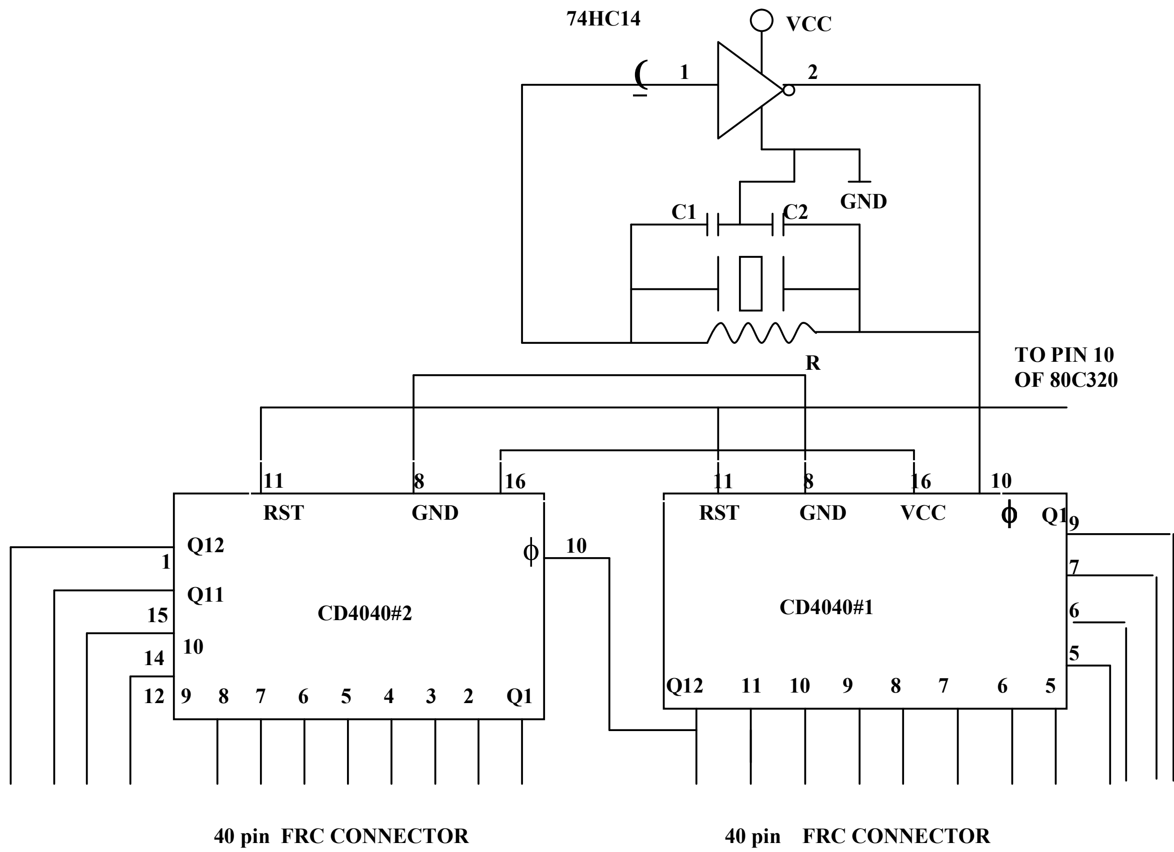

Figure 3.4-V Quartz Crystal Oscillator and frequency counter design

8255 PIN NUMBERS	40 pin FRC CONNECTOR pin	4040 PIN MUMBERS
PA 0 (4)	1	Q1 (9)
PA 1 (3)	2	Q2 (7)
PA 2 (2)	3	Q3 (6)
PA 3 (1)	4	Q4 (5)
PA 4 (40)	5	Q5 (3)
PA 5 (39)	6	Q6 (2)
PA 6 (38)	7	Q7 (4)
PA 7 (37)	8	Q8 (13)
PB 0 (18)	17	Q1 (9)
PB 1 (19)	18	Q2 (7)
PB 2 (20)	19	Q3 (6)
PB 3 (21)	20	Q4 (5)
PB 4 (22)	21	Q5 (3)
PB 5 (23)	22	Q6 (2)
PB 6 (24)	23	Q7 (4)
PB 7 (25)	24	Q8 (13)
PC 0 (14)	16	Q9 (12)
PC 1 (15)	15	Q10 (14)
PC 2 (16)	14	Q11 (15)
PC 3 (17)	13	Q12 (1)
PC 4 (13)	12	Q9 (12)
PC 5 (12)	11	Q10 (14)
PC 6 (11)	10	Q11 (15)
PC 7 (10)	9	Q12 (1)
	25—GND	
	26—VCC	

Table 3.1 FRC connector details

3.4.2.4 MAX232 interface

IC MAX232 is used as in interface IC to communicate the TTL level on TXD and RXD pins of 80C320 into RS232 compatible levels. Please refer to Figure.3.4-VI.

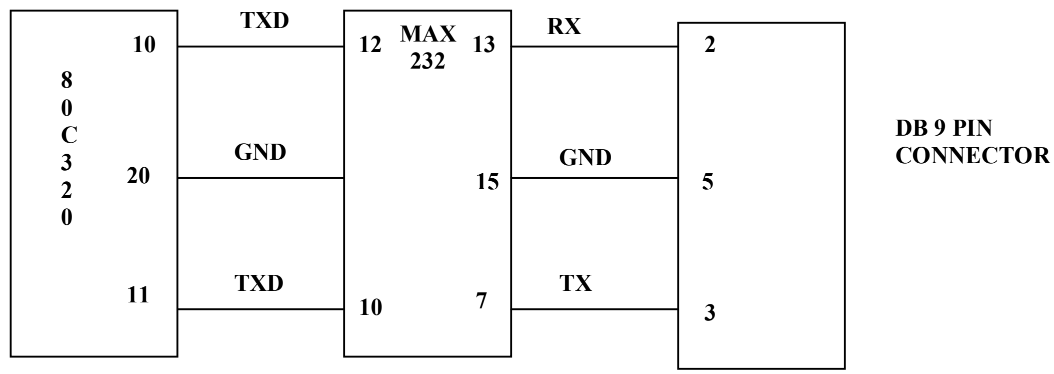

Figure 3.4-VI: RS232 serial Interface between 80C320 and DB9 pin connector of PC

All port lines of 80C320 controller and three ports of IC8255 are engaged for specific required job, no port line was left for interfacing key /s. Programming is done in a such a way that on Power ON, the LCD displays the message "QCM frequency" and frequency measurement starts. A separate key connector is provided for LPC2148 microcontroller based hardware design as explained in 3.4.3

3.4.3 LPC2148 based microcontroller hardware design

Advanced RISC Microcomputer chips were designed by ARM USA based company which are 32 bit microcontrollers. ARM core design was made available to different companies such as Phillips, Atmel to design their own 32 bit ARM controllers with their add on peripheral on chip. The ARM architecture is based on Reduced Instruction Set Computer (RISC) principles, and the instruction set and related decode mechanism are much simpler than those of micro programmed Complex Instruction Set Computers (CISC). This simplicity results in a high instruction throughput and impressive real-time interrupt response from a small and cost-effective processor core. With all peripherals embedded on chip, the ARM based systems are called as System On Chip (SOC) solutions. For the developed instrument, Phillips LPC2148 ARM7TDMI-S was used to make the QCM controller compact. It is a 32-bit microcontroller from ARM7 family.

3.4.3.1 ARM Features

ARM offers following key features:

- 16-bit/32-bit ARM7TDMI-S microcontroller in a tiny LQFP64 package.
- 8 kb 40 kb of on-chip static RAM and 32 kb to 512 kb of on-chip flash memory.
- 128-bit wide interface/accelerator enables high-speed 60 MHz operation.
- In-System Programming/In-Application Programming (ISP/IAP) via on-chip boot loader software. Single flash sector or full chip erase in 400 ms and programming of 256B in 1ms.
- Embedded ICE RT and Embedded Trace interfaces offer real-time debugging with the on-chip Real Monitor software and high-speed tracing of instruction execution.
- USB 2.0 Full-speed compliant device controller with 2 kb of endpoint RAM. In addition, the LPC2146/48 provides 8 kb of on-chip RAM accessible to USB by DMA.
- One or two (LPC2141/42 vs. LPC2144/46/48) 10-bit ADCs provide a total of 6/14 analog inputs, with conversion times as low as 2.44 μs per channel.
- Single 10-bit DAC provides variable analog output (LPC2142/44/46/48 only).
- Two 32-bit timers/external event counters (with four capture and four compare channels each), PWM unit (six outputs) and watchdog.
- Low power Real-Time Clock (RTC) with independent power and 32 kHz clock input.
- Multiple serial interfaces including two UARTs (16C550), two Fast I2C-bus (400 kbit/s),
- SPI and SSP with buffering and variable data length capabilities.
- Vectored Interrupt Controller (VIC) with configurable priorities and vector addresses.
- Up to 45 of 5 V tolerant fast general purpose I/O pins in a tiny LQFP64 package.
- 60 MHz maximum CPU clock available from programmable on-chip PLL with settling time of 100 μs.

- On-chip integrated oscillator operates with an external crystal from 1 MHz to 25 MHz.
- Power saving modes include Idle and Power-down.
- Individual enable/disable of peripheral functions as well as peripheral clock scaling for additional power optimization.
- CPU operating voltage range of 3.0 V to 3.6 V (3.3 V ± 10 %) with 5 V tolerant I/O pads.

3.4.3.2 Memory Map

The LPC2141/2/4/6/8 incorporates several distinct memory regions, shown in the following figures. Figure 3.4-VII shows the overall map of the entire address space from the user program view point following reset.

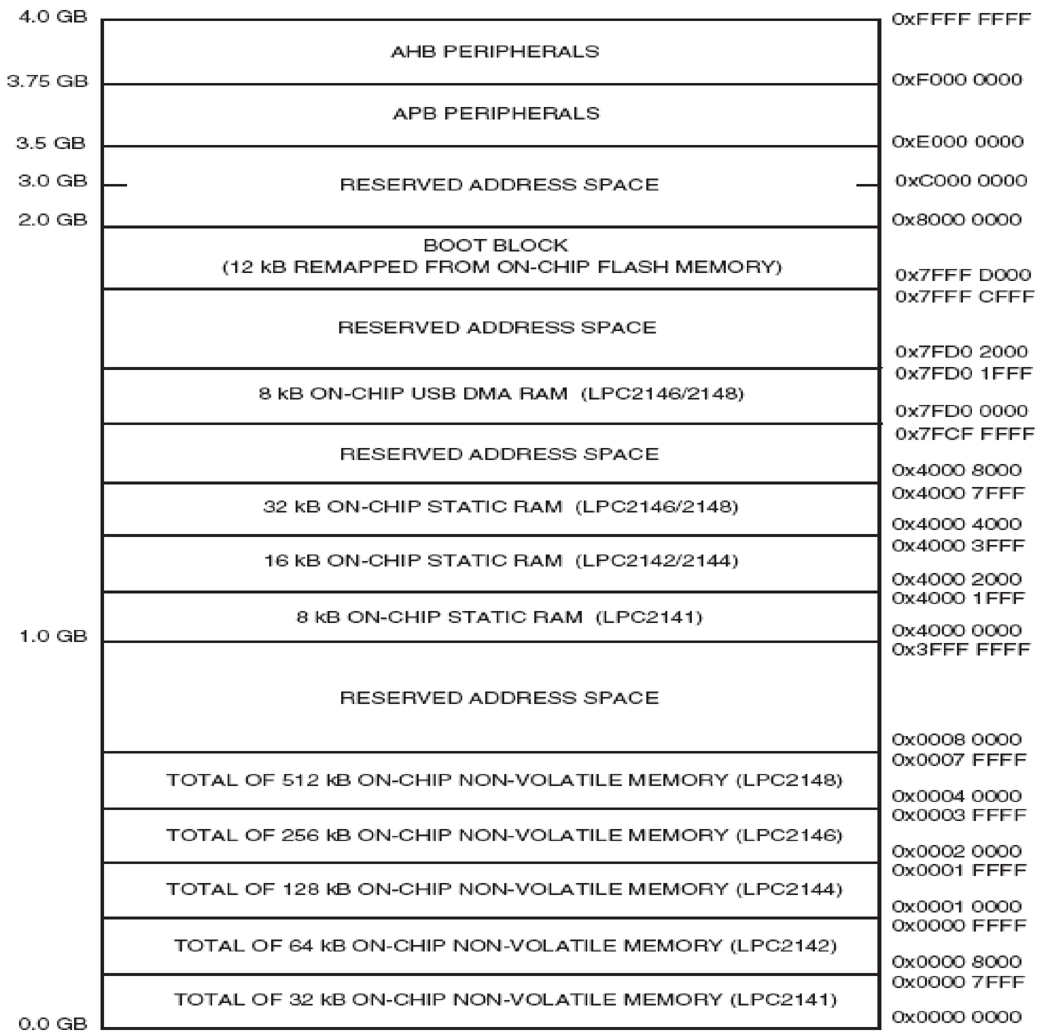

Figure 3.4-VII: Memory map of LPC2148

3.4.3.3. Real Time Clock (RTC)

The RTC is designed to provide a set of counters to measure time when normal or idle operating mode is selected. The RTC has been designed to use little power, making it suitable for battery powered systems where the CPU is not running continuously (Idle mode). The RTC has dedicated 32 kHz oscillator input or clock derived from the external crystal/oscillator input at XTAL1. Please refer to Figure. 3.4-VIII

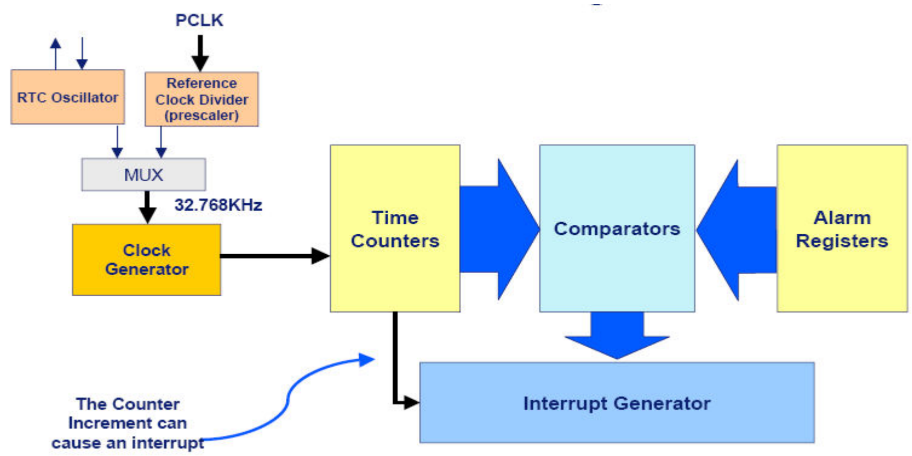

Figure 3.4-VIII – Block diagram of ARM LPC2148 on chip RTC

3.4.3.4 Universal Asynchronous Receiver and Transmitter (UART)

The LPC2148 contains two UARTs. The features of theses UARTs are

- 16 byte Receive and Transmit FIFOs.
- 16-bit baud rate generator clock divisor made from 2 8-bit divisor registers: DLM (MSB), DLL (LSB).Baud rate can be calculated as:

  Required baud rate = pclk/(16 * Divisor)
- Word Length can be selected as: 5, 6, 7 or 8-bit characters.
- Stop Bits can be: 1 or 2 stop bits.
- Parity Select: Odd or Even parity.

3.4.3.5 Phase locked loop (PLL)

There are two PLL modules in the LPC2148 microcontroller. The PLL0 is used to generate the CCLK clock (system clock) while the PLL1 has to supply the clock for the USB at the fixed rate of 48 MHz.The PLL0 and PLL1 accept an input clock frequency in the range of 10 MHz to 25 MHz only. The input frequency is multiplied up the range of 10 MHz to 60 MHz for the CCLK and 48 MHz for the USB clock using a Current Controlled Oscillators (CCO).

3.4.3.6 General purpose I/O ports

LPC2141/2/4/6/8 has two 32-bit General Purpose I/O ports. Total of 30 input/output and a single output only pin out of 32 pins are available on PORT0. PORT1 has up to 16 pins available for GPIO functions.

3.4.3.7 Flash memory system and programming

The flash boot loader provides both In-System and In-Application programming interfaces for programming the on-chip flash memory.

- In-System Programming: In-System programming (ISP) is programming or re-programming the on-chip flash memory, using the boot loader software and a serial port. This can be done when the part resides in the end-user board.
- In Application Programming: In-Application (IAP) programming is performing erase and write operation on the on-chip flash memory, as directed by the end-user application code.

3.4.4 Description of LPC2148 hardware board

The hardware board was designed and developed using LPC 2148 micro-controller with built in ADC, PLL, RTC, UART, Timer/Counter, USB SIE. The other components on this board include MAX 563, 74HC14, LCD & keyboard interface and ISP facility. The on chip flash memory from address locations 0x00010000 to 0x00011000 (8K bytes) is used for data storage. 12MHz crystal is connected to crystal input of LPC2148. On chip RTC is provided with a battery and a 32 KHz crystal. The beauty of this IC is that it has inbuilt In System Programming (ISP) facility so there is no need of an external programmer to download the program code. UART0 of the LPC 2148 is used for ISP. Provision of JTAG interface for flash programming is also made on the board. MAX563 is a dual transceiver with two transmitters and two receivers. It is a 18 pin standard plastic pin DIP. It operates on 3.3V power supply. The MAX563 communicates with RS-232 transceivers, yet consumes far less power; this makes it ideal for battery-powered, hand-held devices. The transmitters are fast with the guaranteed data rate with standard loads is 116kbps, which is the highest rate commonly used by PC-to-PC communication software. LCD interface is provided using GPIO port pins as discussed in 3.4.2.1.

The designed board is shown as in Figure. 3.4-IX and Figure. 3.4-X

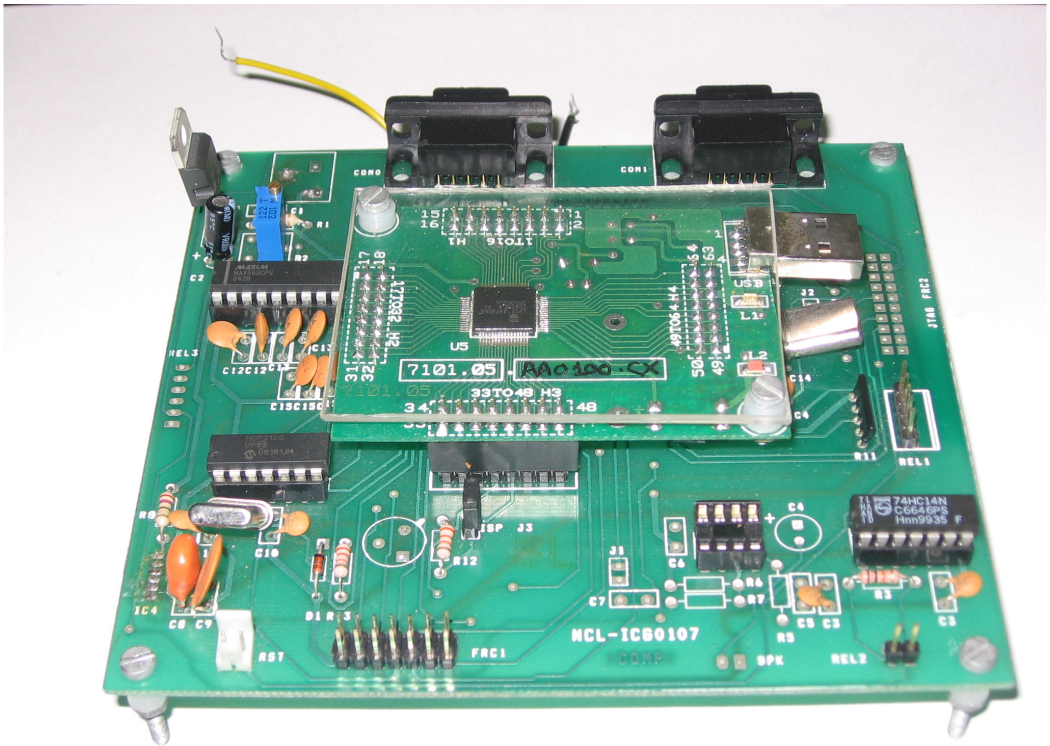

Figure 3.4-IX LPC2148 hardware board showing ARM core

Figure 3.4-X LPC2148 hardware board with LCD and touch keys

LCD interface for LPC2148 is as shown in Table 3.2

LCD connector pin no.	LPC2148 pin no.	Signal definition
7-14	P1.16 - P1.23	DB0-DB7
6	P0.10	Enable
4	P0.11	RS
5	GND	R/W(L)
1	GND	R/W(L)
2	VCC= +5V	
3	GND	Vintensity for maximum intensity

Table 3.2 : Details of interface between LCD connector and LPC2148 pins

Key interface for LPC 2148 is as shown in Table 3.3

LPC 2148 pin no.	Key connector pin no.	Key definition	Key code
P0.20	1	START key	00100000
P0.19	2	STOP key	00080000
P0.18	3	Reserved for future scope	00040000
P0.17	4	Reserved for future scope	00020000
P0.17 – P0.21 port lines are individually pulled up through 10K resistance. A separate RESET key is provided to reset LPC2148.			

Table 3.3 : Details of interface between key connector and LPC2148 pins

On power ON, the QCM controller displays the message “QCM frequency” and waits for START key. On pressing START key, QCM controller starts measuring the QCM crystal frequency. Emergency stop is accomplished by pressing STOP key. The operation can be resumed by RESET key.

IC MAX563 is used for RS232 serial interface between LPC2148 and COM port of PC. Operating voltage of MAX563 is 3.3 V. Please refer to Table 3.4 describing the interface connections for both MAX232 and MAX563 for microcontrollers 80C320 and LPC2148 respectively.

DB 9 PIN connector for PC	**DESCRIPTION DETECTOR**	**MAX 232 PIN NO.**	**MAX 563 PIN NO.**
1	Received line signal (Data carrier detector)		
2	Receiver data	13	15
3	Transmit data	15	13
4	Data terminal ready		
5	Signal ground	7	16
6	Data set ready		
7	Request to send		
8	Clear to send		
9	Ring to indicator		
7,8 – short	1,4,6-short		

Table 3.4: DB9 pin interface connections for MAX232 and MAX563

The designed LPC2148 board is developed as the universal board catering to USB interface, IRDA interface for wireless communication, JTAG interface for downloading the hex codes into on chip Flash memory of LPC2148. These are not used for the developed QCM instrumentation.

CHAPTER 4

DEVELOPMENT OF REAL-TIME SYSTEM SOFTWARE

This chapter describes the assembly and "C" software development done using different development tools for 80C320 microcontroller and ARM LPC2148 microcontroller. It also describes the "C" based software for PC for uploading the data from microcontroller through serial RS232 interface and auto scaling facility for plotting the data on PC.

4.1 Choice of Software

It was decided to use microcontroller as the intelligence for QCM instrument as discussed in Chapter 3. There was a choice to choose assembly programming or to use “C” compilers for 80C31 family microcontrollers for the development of software. Having done extensive assembly programming for couple of projects in the past, it was decided to go for assembly programming to develop real time software for 80C320 - 8 bit microcontroller. For making the instrument compact, Phillips ARM microcontroller LPC2148, 32 bit microcontroller was used for QCM instrument. Real time software was developed using Keil “C” complier as assembly programming for this 32 bit microcontroller was much complicated. “C” language being close to hardware, it was decided to develop “C” based software on PC side for frequency measurement and auto scale facility for plotting.

4.2 Assembly software development for 80C320 based hardware

4.2.1 Development tools used

4.2.1.1 ASM31 assembler by M/s SPJ systems, Pune

The programs were written using 80C320 mnemonics. The Turbo C editor was used to create .asm file. ASM31 assembler created .hex and .prn files when the program was error free. Hex file contains Operational Codes (OPCODE) and required to be fused into EEPROM 27C128 for power on execution. Prn file is a list file for documentation purpose. ASM31 does not provide debugger. Bugs in the program were removed using logic.

4.2.1.2 PC-UPROG - PC based programmer by M/s Dynalog, Pune

PC_UPROG is the universal programmer required to fuse the hex file data into the EEPROM. The programmer contains the add on card to be fitted into the computer which takes care of providing proper programming voltage to fuse the data into EEPROM. The software utility loaded on PC takes care of selection of company, EEPROM number, reading hex file and programming the OPCODEs in the hex file at key control. The PC_UPROG utility is DOS / Windows based.

4.2.1.3 Personal computer for development of assembly programs

A dedicated personal computer was used for development of assembly programs for 80C320 microcontroller hardware. Turbo C editor was used to write and edit the .asm files. ASM31 assembler loaded on PC was used to assemble the TC files. ASM 31 creates .hex and .prn files as stated in 4.2.1.1. PC_UPROG programmer was used to fuse the hex codes into the EEPROM. The programmer talks to PC through PC add on card developed by Dynalog company and its software utility. COM1 / COM2 serial port of the PC was used for uploading the data from 80C320 hardware on PC using serial RS232 protocols via serial cable. PC was also used to develop "C" based software to read the data on COM1 / COM2 for frequency measurement and plotting with auto scale facility.

4.2.2. Assembly routines developed for 80C320 microcontroller hardware

The complete assembly software development for 80C320 hardware includes routines for initialization, LCD display, RTC interrupt, Frequency measurement, serial communication and others. Some important routines are explained below.

4.2.2.1 Initialization routine – This routine initializes first the Stack Pointer to the on chip RAM memory location 70H, clears the on chip memory locations 30H to 4FH allocated for 16x2 LCD display, initializes Port 1 as output port and port 3 is as follows

P3.0 - in alternate definition: as RXD – for receiving data for serial RS232 communication . OR in the output mode as reset control line to reset 4040 decode counters.

P3.1 – in alternate definition – as TXD – for transmitting data for serial RS232 communication

P3.2 – in alternate definition – as INTO(L) - for servicing real time interrupt coming from RTC DS1287 chip.

P3.3 – as output line for chip select signal of RTC DS1287 chip

P3.4 – as output pin – RS control pin of LCD

P3.5 – as output pin – Enable control pin of LCD

P3.6 – in alternate definition –as WR(L) signal for WRITE operations for 8255 chip.

P3.7 – in alternate definition – as RD(L) signal for READ operations for RTC and 8255 peripherals.

Port A, Port B and Port C of 8255 are configured as input ports. The register A of RTC DS1287 is configured to issue interrupt every after 500 miliseconds (ms).

4.2.2.2. LCD routine: It takes care of displaying 32 characters (ASCII codes of characters) stored in on chip RAM location 30H-4fh of 80C320 to 16x2 LCD display.

4.2.2.3 RTC_ISR routine:: This is the interrupt service routine and is executed when RTC issues low signal on IRQ pin after 500 ms which makes the INTO(L) pin of 80C320 low. INTO(L) being vector addressed interrupt of 80C320, on receiving low voltage level on INTO(L), the program jumps 0003H memory location where the jump is made to RTC_ISR. The first instruction in this ISR is to read "C" register of RTC chip so that the IRQ low output is made high. A software RTC flag is made high and routine is returned. The main program constantly checks for high state of RTC flag. When the condition is true, first the flag is made low to service next interrupt. One more RTC2 flag is used to differentiate between even and odd number of interrupts. For odd number of interrupts RTC2 flag is set to zero and for even number of interrupts RTC2 flag is set to one. This flag is checked in the main routine for making the decision for displaying the frequency value. Please refer to Figure. 4.1 For "count" period, RTC2 flag is set to zero. For "display" period. RTC2 flag is set to one.

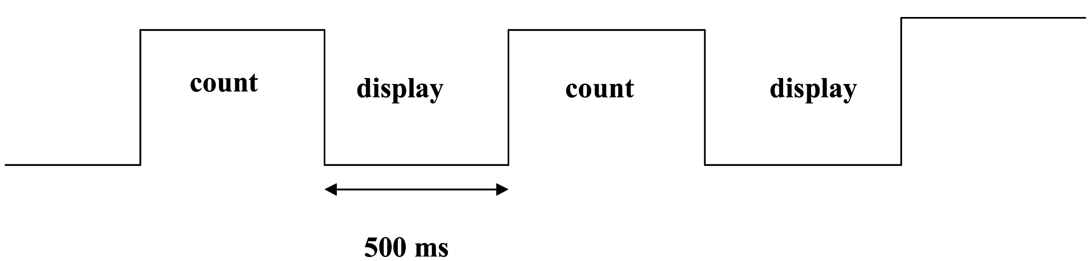

Figure. 4.1 RTC_ISR logic

4.2.2.4 Freq_read: This routine is responsible to read the Quartz crystal frequency. When main routine checks for RTC flag high, routine then checks for RTC2 flag status. If status of RTC2 flag is zero, the active high reset pulse is issued on RESET pin of 4040 decade counter chip. Please refer to Fig. 3.4 V Due to this counting of the pulses by two decade counters is initiated. When the status of RTC flag is one, the control goes to Freq_read routine. It reads the counted number of pulses by reading Port A, Port B and Port C of 8255. Please refer to Fig. 3.4 V and Table 3.1. Q1 to Q12 outputs of decade counters are connected to three ports of 8255. The hex frequency value is stored in the temporary registers. Then active high reset pulse is issued on RESET control pin of decade counter to count frequency value for next second.

4.2.2.5 Serial_RT: This routine takes care of uploading the measured frequency to PC through serial RS232 protocols. The methodology is as explained below.
Serial asynchronous communication is used to upload the data. PC waits for Start code "S" which is transmitted by 80C320 before sending six byte data. Once this Start code is received on PC, the computer assumes that next six bytes coming on serial port is six bytes data. This data is the frequency measurement done for 500 ms period. So, the data is multiplied by 2 and is plotted which is explained in Figure. 4.1.

4.3 Software development for LPC2148 ARM core hardware

4.3.1 Development tools used

4.3.1.1 <u>Keil Microvision 3 by M/s Keil, Germany</u>

This is a PC based development tool. The software development for LPC 2148 hardware has been completed using Keil "C" compiler of Keil Microvision 3 by Keil, Germany. LPC 2148 being ARM7 core for 32 bit microcontroller, it was not easy to develop the software using assembly programming for LPC2148 hardware. The programs were developed in embedded "C" using editor tool of Keil Microvision 3 and the same was optimized and complied by using compiler tool of Keil Microvision 3. After error free compilation, .hex file is generated which are nothing but the executable hex code for LPC2148 core.

4.3.1.2 LPC2000 Flash Utility V2.2.3

LPC2000 Flash Utility is a PC based development tool. This utility downloads the hex file generated after error free compiled programs as stated in 4.3.1.1 into the on chip Flash EEPROM of LPC2148. The utility is developed by Phillips company for Phillips ARM cores. It is nothing but the programmer tool as explained in 4.2.1.2. The hex codes are downloaded through serial RS232 communication. Serial cable was connected between COM2 serial port of PC and 9 pin serial UART2 connector on developed LPC2148 hardware. On LPC 2000 utility, COM2 port was selected and other parameters for serial communication used were 9600 baud rate, 8 data bits, 1 stop bit and no parity. On developed LPC2148 hardware, In Circuit Programming (ICP) hardware was developed to receive the data coming from PC through UART2 port. Through LPC2000 utility, the downloaded data is programmed / fused into Flash EEPROM of LC2148 ARM core.

4.3.2 "C" routines developed for LPC2148 ARM core.

The same logic is used for development of "C" programs for Initialization routine, LCD routine, Serial RT routine as explained in 4.2.2.1, 4.2.2.2 and 4.2.2.5. ARM core used has on chip RTC hardware. It is programmed to generate an on chip software interrupt every after one second. On interrupt control goes to RTC_ISR routine where the frequency count value is read and stored in temporary registers. For reading frequency pulses, ARM hardware does not use decade counters and PPI 8255. The crystal oscillator output is directly connected to the P0.28 pin of LPC2148 which is programmed as counter 0 pin.

4.4 Software development on PC using "C" language

The high level language program was developed on using "C" language for following purposes.

a. Reading the frequency value from 80C320 microcontroller / LPC2148 ARM core through serial RS232 communication. PC COM2 port is sued for this purpose. The serial parameters were programmed as 9600 baud rate, 8 data bits, 1 stop bit and no parity. While reading the data, first program waits for Start code “S”. When this code is received, next six bytes are read and stores as six bytes of frequency value.

b. Real time plotting of the frequency value with auto scale facility.

The graphical mode commands were set for PC monitor screen. X axis was plotted for “Second” parameter. One pixel on X axis is treated for one second reading. Y axis was plotted for frequency value. The program was written for auto scaling of Y axis as per the current frequency value. Program constantly updates the current frequency value on PC monitor screen. Maximum number of seconds for which frequency value gets plotted were 24 x 60 x 60 seconds.

c. File storage: The frequency value and corresponding second value are stored in the file. The type of the file is text file. The name of the file can be given by user and then it is saved as .TXT file. This file can be used by user for further data processing.

CHAPTER 5

EXPERIMENTAL RESULTS AND ANALYSIS

This chapter covers the different experiments that were studied with the developed QCM instrument.

5.1 Design Validation Experimentation

Design validation of the developed QCM was done by first observing the damping effect with pure water and HPLC grade methanol. For all the experimentation in this thesis we have used AT cut gold coated 9MHz quartz crystal. As soon as a drop of water is placed on crystal surface by syringe, the frequency reading on LCD was reduced to 2MHz. Then on another crystal, HPLC grade methanol drop was placed on crystal surface. A damping effect in terms of frequency was observed on LCD. During next few seconds, as methanol started evaporating, the frequency reading on LCD increased and finally when full evaporation of methanol took place, crystal regained its original frequency.

The first in – situ test was carried out for entrapment of silver ions in organic thin films deposited on crystal surface. For this, firstly the bare crystal frequency reading was noted down. Then pentadecylphenol (PDP) film of 200 nm thickness was deposited on the crystal surface using Edwards vacuum coating unit available with the Nanoscience group, NCL. With PDP film deposited on crystal, the frequency of the same crystal was noted again. The frequency was reduced and the difference noted was about 1000 Hz. Then the liquid sample (silver ion sample) prepared by the Nanoscience group was poured on crystal surface. Immediate damping of the frequency was observed on PC and frequency was reduced to about 0.9 MHz. For about 900 seconds there were small variations in frequency showing the silver ions getting entrapped in the PDP film. After that there was increase in the frequency upto 1.25 MHz and system became stable.

Fully developed QCM instrumentation was tested for kinetics of frequency measurements. Imported NIMA Langmuir Blodgett trough (Model 611D), available with the Nanoscience group at NCL, was used for this measurement. LB films of standard Octadecylamine (ODA) surfactant were deposited on the QCM crystals. Pressure–area (π–A) isotherms were recorded at room temperature as a function of time from spreading the monolayer at a compression and expansion rate of 100 cm^2/min. A standard Wilhelmy plate was used for surface pressure sensing. From the π–A isotherm measurements , a region of large incompressibility is seen to occur up to surface pressure of 20 mN/m and therefore, multilayer films of ODA monolayer were transferred onto gold-coated quartz crystals at this surface pressure by the LB technique at a constant surface pressure with a deposition rate of 20 mm/min with a waiting time of 60s between dips on gold-coated AT-cut quartz crystals for QCM measurement. The frequency change during formation of multilayer of ODA by LB technique was studied by QCM and the data obtained is shown in Figure. **5.1** It can be seen from the QCM measurements that the frequency change is nearly constant during each deposition. This indicates that the ODA monolayers are transferred onto the substrate uniformly in a layer-by-layer fashion.

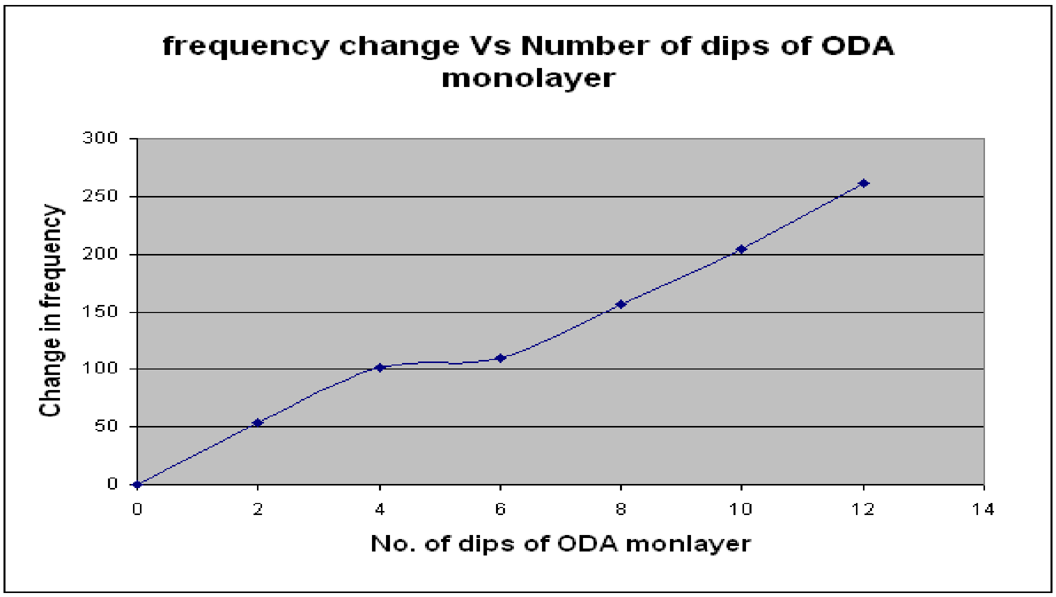

Figure 5.1 Frequency change Vs number of dips of ODA monolayer

Few other systems were studied on the developed QCM instrumentation. The samples for experimentation were provided by the Nanoscience group at NCL. For LB film deposition on quartz crystal, Langmuir Blodgett trough (model 611D) was used.

5.2 Experimentation I

Kinetic measurement study of Octadecylamine (CH_3-$(CH_2)_{17}$-NH_2 - Aldrich) monolayer on different subphases:

5.2.1 ODA on Chloroauric acid ($HAuCl_4$)

QCM crystal was fixed in the dipper mechanism assembly of NIMA LB trough. The PC user interface for NIMA was set for one cycle with a waiting time of 60 seconds for QCM measurement. One cycle is of one dip i.e. first dipper mechanism goes down and by that dipping the crystal in the solution and then making the dipper mechanism up, by that taking crystal out of solution spread on the trough. For further referred tables and graphs, one cycle is referred as these two operations.

200 µL of ODA in chloroform (concentration 1 mg/mL) was spread on the surface of 10^{-4} M aqueous chloroauric acid ($HAuCl_4$) solution in a Langmuir trough. After measurement of π–A isotherms, the ODA monolayer was compressed to a surface pressure of 25 mN/m and maintained at this pressure. The amine groups of ODA spread on the aqueous $HAuCl_4$ solution are protonated and thus electrostatically complex with chloroaurate anions $(AuCl_4)^-$ present in the subphase. The complexation of $(AuCl_4)^-$ ions with ODA monolayer leads to the organization of the monolayer at the air-water interface. Please refer to Figure. 5.2.1-I. These monolayers were transferred onto gold-coated quartz crystals at this surface pressure by the LB technique with a deposition rate of 20 mm/min with a waiting time of 60 seconds for QCM measurement. Every after one dip, the frequency change was measured.

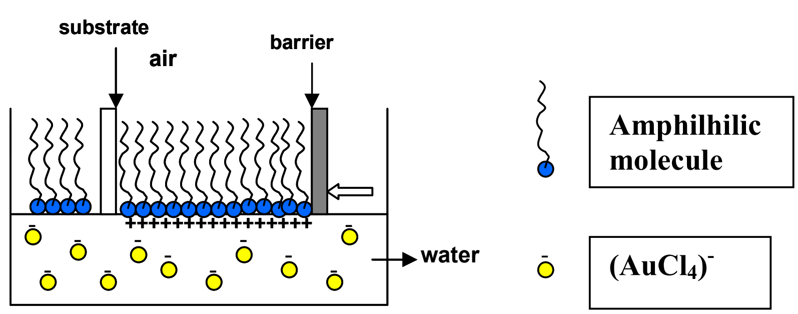

ODA – An Amphiphilic molecule showing hydrophobic tail (long hydrocarbon chain) and hydrophilic head (polar group)

Figure 5.2.1-I ODA – an amphiphilic molecule

Data obtained for this experimentation is shown in Table 5.2.1-I and Figure. 5.2.1-II & Figure. 5.2.1-III

No.of dips	Δ f	Δ m= Δf / 0.181
1	68	375.6
2	168	917.12
3	256	1414.36
4	344	1900.55
5	428	2364.64
6	528	2917.12

Table 5.2.1-I Experimental data for ODA on Chloroauric acid ($HAuCl_4$)

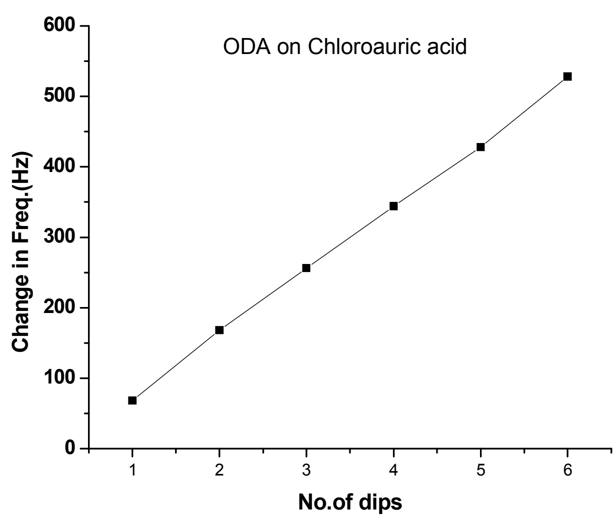

Figure 5.2.1-II – ODA on Chloroauric acid ($HAuCl_4$)

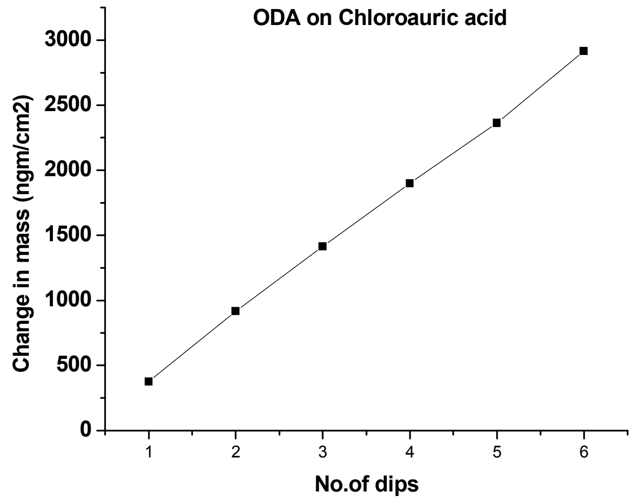

Figure 5.2.1-III ODA on Chloroauric acid ($HAuCl_4$)

The frequency change on deposition of the film can be converted to mass loading by using the Saurbrey formula [7].

$$\Delta f = -\,2\, f_o^{\,2} \times \frac{\Delta m}{A \times (\mu \times \rho)^{1/2}}$$

where Δf - frequency change, f_o - frequency of the crystal prior to a mass change, Δm - mass change, A - Piezo electrically active area, μ - shear modulus for quartz, ρ - density of quartz ($\mu = 2.95 \times 10^{11}$ g cm^{-1} s^{-2}, $\rho = 2.65$ g/cm^3).

Sauerbrey equation can be written as $\Delta f = \Delta m * C_f$

For 9 MHz AT cut Quartz crystal used for experimentation, C_f= 0.181

Number of ions uptake for every dip has been calculated

Following are the calculation for the mass uptake of a monolayer for one cycle.

Molecular area of ODA molecule is 20 A^{0^2} / molecule.

Number of ODA / molecule = 1 / $(20 \times 10^{-16}) = 5 \times 10^{14}$

Molecular weight of ODA is 269.52

This means 269.52 gms of ODA contains 6.023 x 10^{23} molecules of ODA

So, 5 x 10^{14} molecules of ODA contains

(269.52 x 5 x 10^{14}) / 6.023 x 10^{23} = 223 ngms / cm^2 of ODA.

Molecular weight of $AuCl_4^-$ is 339.7

This means 339.7 gms of $AuCl_4^-$ contains 6.023 x 10^{23} molecules of $AuCl_4^-$

So, 5 x 10^{14} molecules of ODA contains

(339.7 x 5 x 10^{14}) / 6.023 x 10^{23} = 280 ngm / cm^2 of $AuCl_4^-$

Therefore, change in the mass uptake of a monolayer during one cycle operation is

Δ m = Δ m ODA + Δ m $AuCl_4^-$

= 223 + 280 = 503 ngm / cm^2

Thus for one cycle , mass uptake is 503 ngm / cm^2

Every one molecule of ODA interacts with one molecule of $AuCl_4^-$

From Figure 5.4, slopes are calculated for every cycle change. These are 542.12, 497.24, 486.19, 464.09, 552.48 ngm/cm^2.

It is observed that the mass uptake is almost equal for every monolayer deposited on quartz crystal which is very close to theoretical calculations of 503 ngm/cm^2.

5.2.2 ODA on Potasium Hexaflurotitanate (K_2TiF_6)

200 µL of ODA in chloroform (1 mg/mL concentration) was spread on the surface of 10^{-4} M aqueous Potasium Hexaflurotitanate (K_2TiF_6) solution in a Langmuir trough. After measurement of π–A isotherms, the ODA monolayer was compressed to a surface pressure of 25 mN/m and maintained at this pressure. The amine groups of ODA, spread on the aqueous K_2TiF_6 solution are protonated and thus electrostatically complex with $TiF6^{2-}$ present in the subphase and forms Lamgmuir monolayer at air water interface. These monolayer were transferred onto gold-coated quartz crystals at this surface pressure by the LB technique with a deposition rate of 20 mm/min with a waiting time of 60 seconds for QCM measurement. Every after one dip, frequency change was measured. Data obtained for this experimentation is shown in Table 5.2.2-I and Figure. 5.2.2-I & Figure. 5.2.2-II.

Change in the mass per cycle has been calculated using Sauerbrey equation. Number of ions uptake for every cycle has been calculated and it is observed that every one molecule of ODA interacts with two molecule of $TiF6^{2-}$ and the mass uptake is almost equal for every monolayer deposited on quartz crystal.

No.of dips	Δ f	Δ m= Δf / 0.181
2	1252	6917
4	1729	9552
6	2276	12574
8	2528	13966
10	3128	17281
12	3170	17513
14	3702	20452
16	4116	22741
18	5100	26175

Table 5.2.2-I Experimental data for ODA on Potasium Hexaflurotitanate (K_2TiF_6)

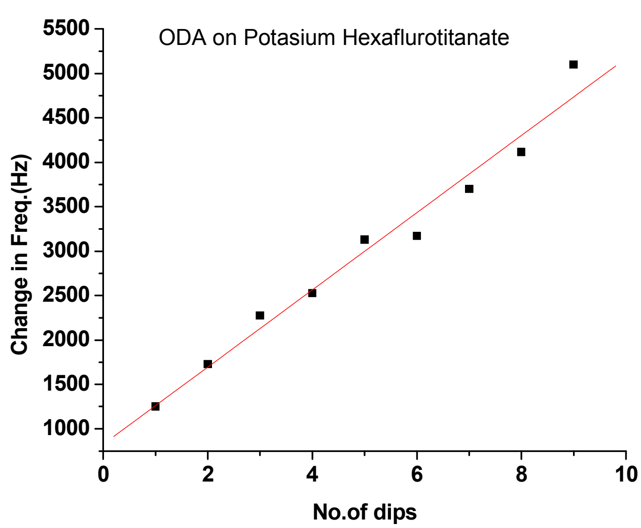

Figure 5.2.2-I - ODA on Potasium Hexaflurotitanate

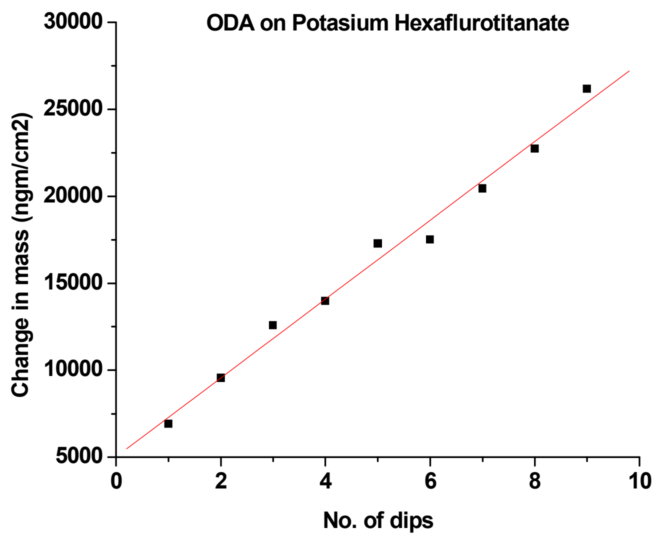

Figure 5.2.2-II ODA on Potasium Hexaflurotitanate

5.2.3 ODA on chloroplatenic acid (H_2PtCl_6)

200 µL of ODA in chloroform (1 mg/mL concentration) was spread on the surface of 10^{-4} M aqueous chloroplatenic acid (H_2PtCl_6) solution in a Langmuir trough. After measurement of π–A isotherms, the ODA monolayer was compressed to a surface pressure of 25 mN/m and maintained at this pressure. The amine groups of ODA, spread on the aqueous H_2PtCl_6 solution are protonated and thus electrostatically complex with $PtCl_6^-$ present in the subphase and forms Langmuir monolayer at air water interface. These monolayer were transferred onto gold-coated quartz crystals at this surface pressure by the LB technique with a deposition rate of 20 mm/min with a waiting time of 60 seconds for QCM measurement. Every after once dip, frequency change was measured. Data obtained for this experimentation is shown in Table 5.2.3-I and Figure. 5.2.3-I & Figure. 5.2.3-II.

No.of dips	Δ f	Δ m= Δf / 0.181
2	412	2276
4	476	2629
6	540	2983
8	596	3303
10	608	3348
12	616	3402
14	626	3458

Table 5.2.3-I Experimental data for ODA on chloroplatenic acid (H_2PtCl_6)

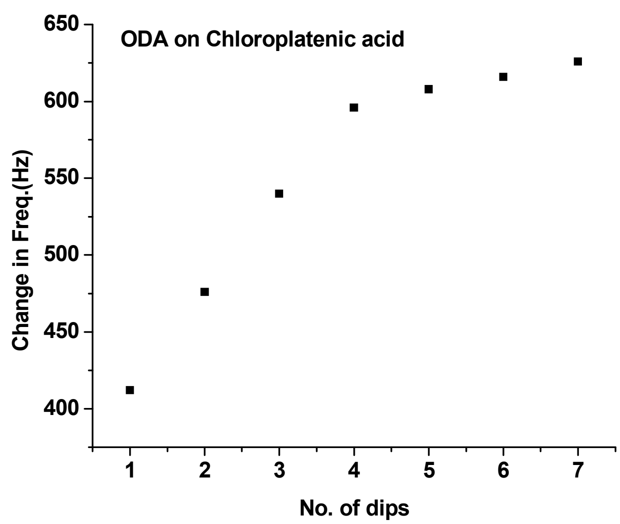

Figure 5.2.3-I ODA on chloroplatenic acid (H_2PtCl_6)

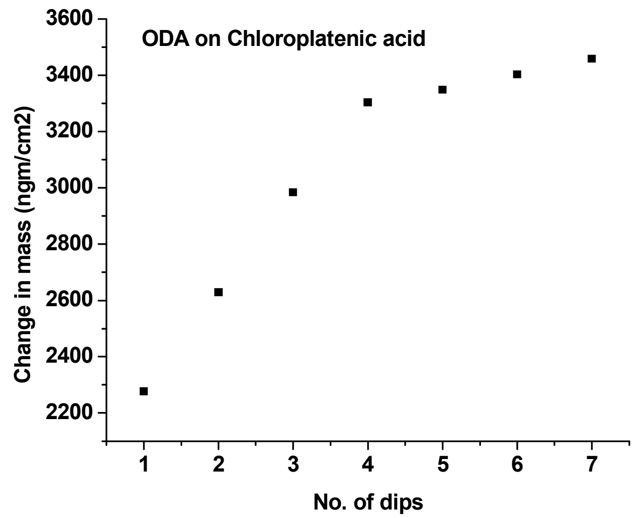

Figure 5.2.3-II ODA on chloroplatenic acid (H_2PtCl_6)

It is observed that for first four dips, the change in mass was linearly increasing. This means LB film was deposited properly on the QCM crystal. After four dip, film deposition was not good.

With Sauerbrey equation change in mass has been calculated. Number of ions uptake for every dip has been calculated. It is observed that every one molecule of ODA interacts with two molecule of $PtCl_6^-$ and the mass uptake is almost equal for every monolayer deposited on quartz crystal for first four dips.

5.3 Experimentation II

Time dependent complexation of sodium borohydride reduced gold nanoparticles on octadecylamine Langmuir monolayers for in situ QCM measurement

In-situ QCM measurement were carried for studying time dependent complexation of sodium borohydride reduced gold nanoparticles on octadecylamine Langmuir monolayers. The developed flow cell (Ref. Chapter3: Section 3.3) was used for this experimentation.

Experimental section:

In a typical experiment, 100 mL of 10^{-4} M aqueous solution of chloroauric acid was reduced by 0.01 g of sodium borohydride at room temperature, which resulted in a ruby-red solution indicating the formation of gold nanoparticles [ref]. The solution was kept for 24 hour and the P_H around 5.6 was measured. This gold nanoparticle solution

(400µl) was applied on the different film thickness (4 and 6 dips) of ODA deposited surface of QCM crystal using LB technique. Frequency changes were measured for nearly for 3Hrs 50min.

Data obtained is shown in Figure 5.3-I and Figure 5.3-II.

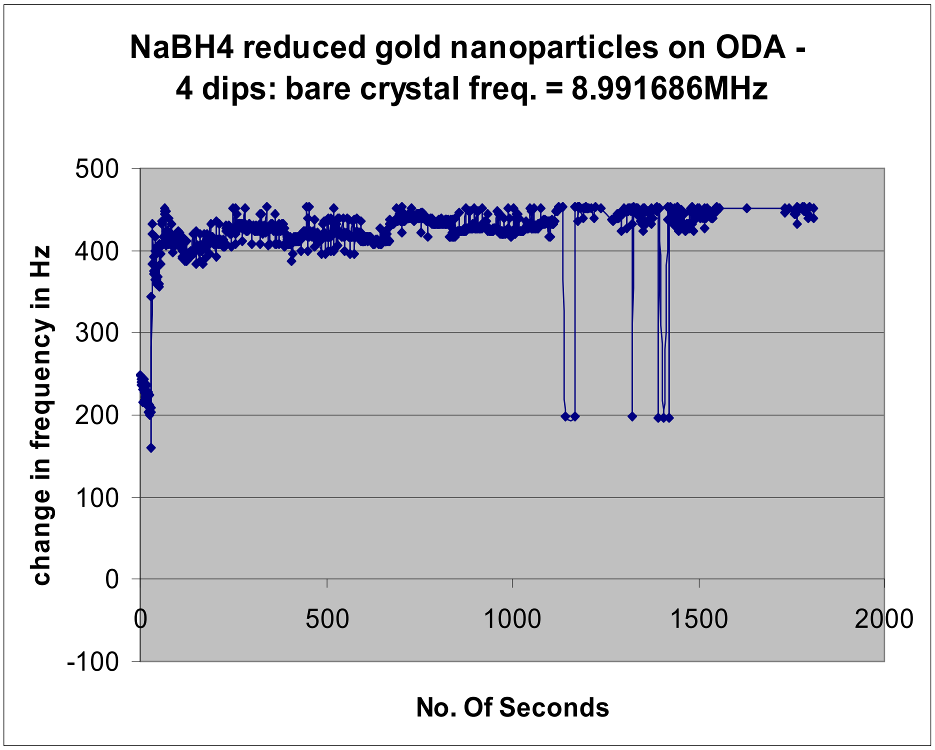

Figure 5.3-I Time dependent complexation of sodium borohydride reduced gold nanoparticles on octadecylamine Langmuir monolayers.

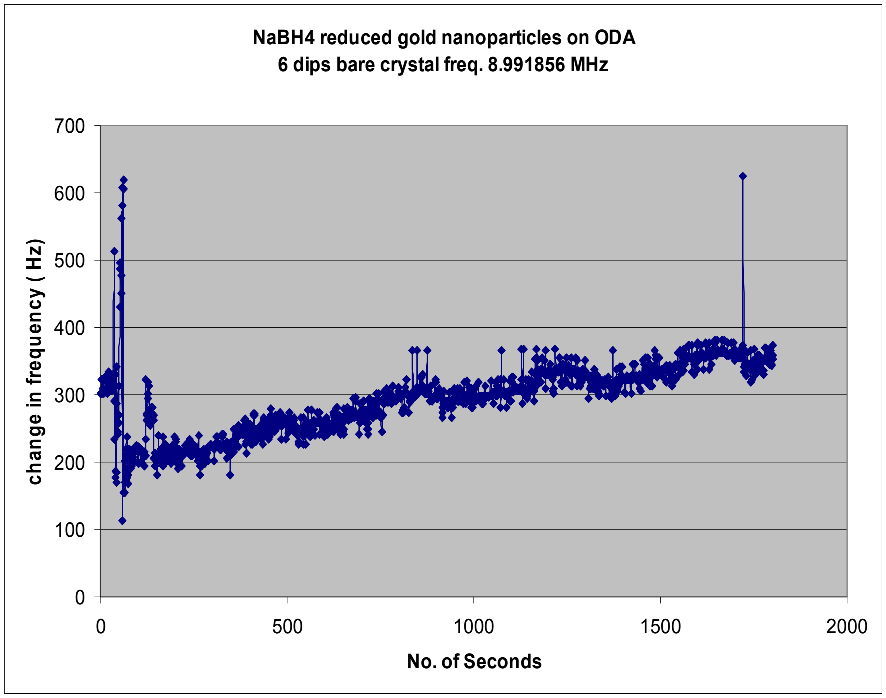

Figure 5.3-II Time dependent complexation of sodium borohydride reduced gold nanoparticles on octadecylamine Langmuir monolayers.

From the experiments carried out using NIMA LB trough for deposition of monolayers on QCM crystals as explained in Experimentation I – 5.2.1, 5.2.2, 5.2.3, it is cleared that the theoretical calculations of mass uptake during every dip is very close to the value calculated by doing experiments. This is the important feedback for the material characterization and useful to Material Scientists to pursue further research.

CHAPTER 6

CONCLUSIONS

This chapter covers the salient features of the work detailed in the thesis and the possible avenues for future work.

The developed QCM instrument is an indigenous development to study molecular recognition processes in lipid films. While designing the instrument, a detailed study of commercially available instruments has been taking into consideration. The developed instrument is compact, economical and can be called as Embedded System. The instrument includes System On Chip (SOC) hardware for frequency measurement and uploading the data to PC through RS232 interface. Instrument incorporates flow cell for in-situ measurements in liquid medium. Real time system software has been developed for frequency measurement, display and keyboard controls, serial RS232 communication protocols, plotting of frequency measured with auto scale facility. Following criteria have been used to make the instrument economical and user friendly.

1. Automatic frequency measurement at a key command. The instrument is not designed for a particular frequency.
2. Microcontroller is used as the intelligence for frequency measurement.
3. System On Chip (SOC) solution is implemented by using ARM core based development to make the instrument compact to call it as Embedded System. The instrument can be used on 230V mains voltage or battery operated.
4. Frequency measurement range up to 10 MHz.
5. User friendly real time software using ARM core for frequency measurement.
6. User friendly real time software using "C" language for uploading data from ARM core, plotting with auto scale and file storage.

QCM specifications

Frequency range: up to 10 MHz

Frequency resolution: 1 Hz

Display: 16 X 2 Oriole LCD display

Key board: touch keys

Computer interface: serial RS232 interface

Maximum time for in-situ measurement: 24 hours

Power supply: mains voltage 230V, 50 Hz
Battery operation: 3.3V

QCM crystal:

Frequency: 9 MHz, AT cut Diameter: 1 inch

Surface finished: Polished

Electrode material: 100 A^0 Cr / 1000 A^0 Au

Blank diameter: 0.538 inch Electrode diameter: 0.201 inch

Mounted and bonded to HC-48/U base

Flow Cell: 100µl capacity, suitably designed to fix one inch diameter QCM crystal

Software:

ARM based firmware for real time frequency measurement and RS232 communication, display and keyboard controls

"C" based user friendly real time software for receiving frequency value through RS232, plotting with auto scale and file storage for post processing.

Future Scope:

The developed QCM instrument can measure frequency up to 30 MHz. The SOC solution and the present firmware developed has capability to measure frequency up to 30 MHz. In near future the small interface work on ARM hardware will be completed to measure frequency up to 30 MHz. USB interface in addition to serial RS232 interface can be incorporated. With the ARM9 core as the basic intelligence, the firmware can be developed for incorporating an internet communication feature in the QCM embedded module. At a key stroke, the data acquired can be sent through internet on the required host address. LabVIEW based user friendly software can be developed on PC side for frequency measurement through serial RS232 interface with required Graphical User Interface. Using LabVIEW software, additional and important feature of web publishing of real time data can be incorporated. Due to this utility, on going experimental data can be viewed by the Project Leader and team members on their desktops.

Appendix A – Data Sheets

Phillips LPC2141/42/44/46/48

Single-chip 16-bit/32-bit microcontrollers; up to 512 kB flash with ISP/IAP, USB 2.0 full-speed device, 10-bit ADC and DAC

General description

The LPC2141/42/44/46/48 microcontrollers are based on a 16-bit/32-bit ARM7TDMI-S CPU with real-time emulation and embedded trace support, that combine microcontroller with embedded high-speed flash memory ranging from 32 kB to 512 kB. A 128-bit wide memory interface and a unique accelerator architecture enable 32-bit code execution at the maximum clock rate. For critical code size applications, the alternative 16-bit Thumb mode reduces code by more than 30 % with minimal performance penalty. Due to their tiny size and low power consumption, LPC2141/42/44/46/48 are ideal for applications where miniaturization is a key requirement, such as access control and point-of-sale. Serial communications interfaces ranging from a USB 2.0 Full-speed device, multiple UARTs, SPI, SSP to I2C-bus and on-chip SRAM of 8 kB up to 40 kB, make these devices very well suited for communication gateways and protocol converters, soft modems, voice recognition and low end imaging, providing both large buffer size and high processing power. Various 32-bit timers, single or dual 10-bit ADC(s), 10-bit DAC, PWM channels and 45 fast GPIO lines with up to nine edge or level sensitive external interrupt pins make these microcontrollers suitable for industrial control and medical applications.

Pinning Diagram:

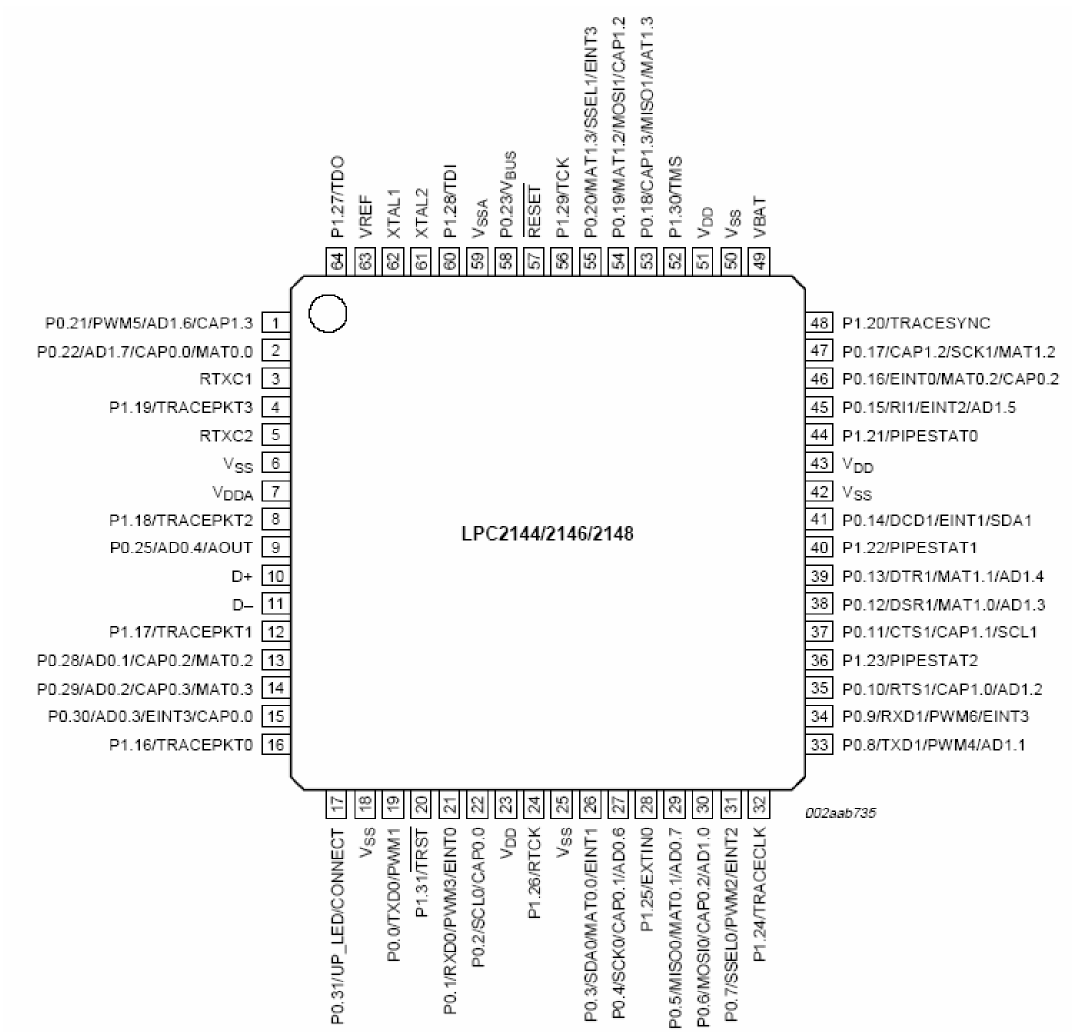

Block Diagram:

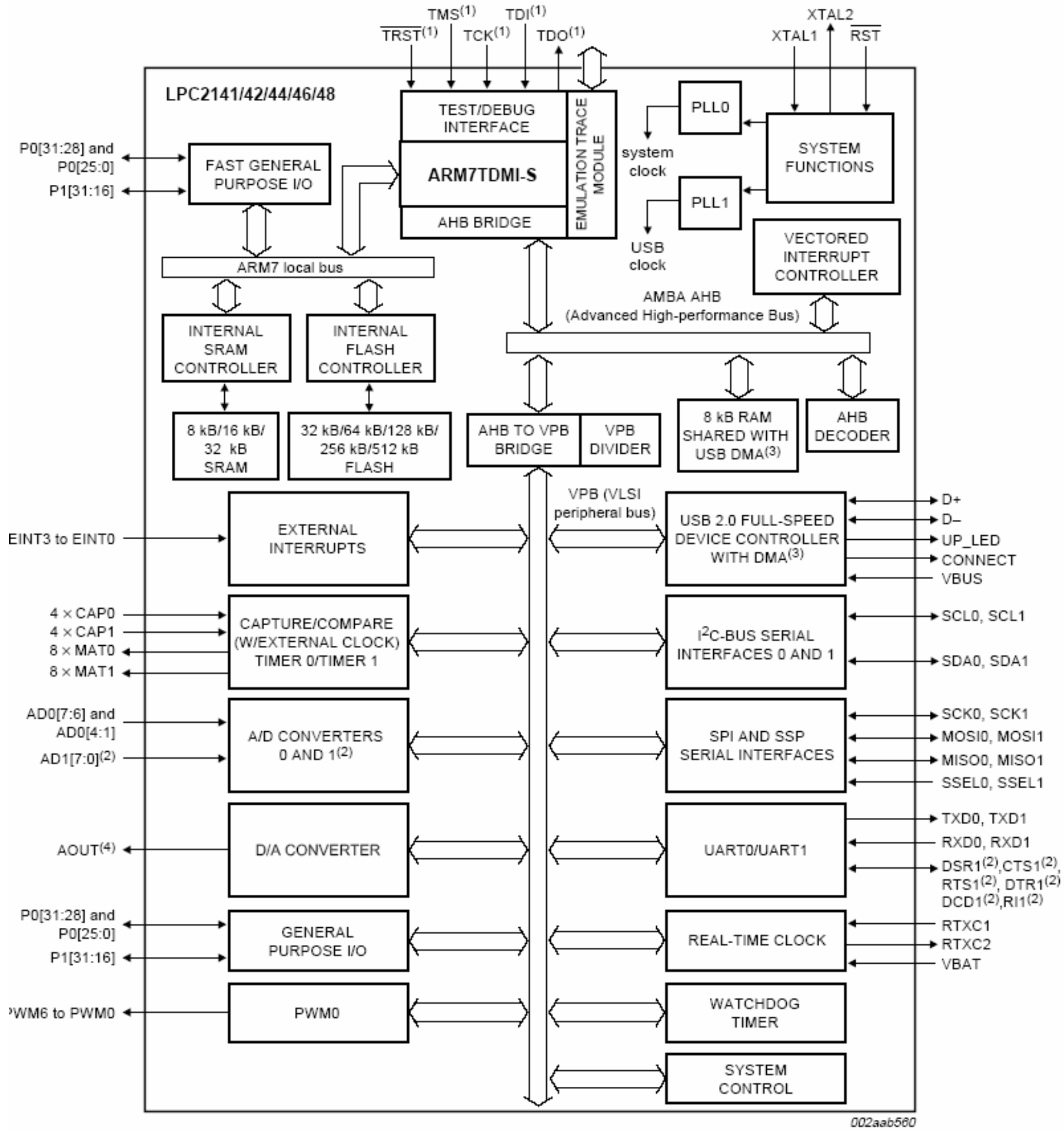

(1) Pins shared with GPIO.

(2) LPC2144/46/48 only.

(3) USB DMA controller with 8 kB of RAM accessible as general purpose RAM and/or DMA is available in LPC2146/48 only.

(4) LPC2142/44/46/48 only.

Pinning details:

Symbol	Pin	Type	Description
P0.0 to P0.31		I/O	**Port 0:** Port 0 is a 32-bit I/O port with individual direction controls for each bit. Total of 31 pins of the Port 0 can be used as a general purpose bidirectional digital I/Os while P0.31 is output only pin. The operation of port 0 pins depends upon the pin function selected via the pin connect block. Pins P0.24, P0.26 and P0.27 are not available.
P0.0/TXD0/ PWM1	19[1]	I/O	**P0.0 —** General purpose input/output digital pin (GPIO).
		O	**TXD0 —** Transmitter output for UART0.
		O	**PWM1 —** Pulse Width Modulator output 1.
P0.1/RXD0/ PWM3/EINT0	21[2]	I/O	**P0.1 —** General purpose input/output digital pin (GPIO).
		I	**RXD0 —** Receiver input for UART0.
		O	**PWM3 —** Pulse Width Modulator output 3.
		I	**EINT0 —** External interrupt 0 input
P0.2/SCL0/ CAP0.0	22[3]	I/O	**P0.2 —** General purpose input/output digital pin (GPIO).
		I/O	**SCL0 —** I^2C0 clock input/output. Open-drain output (for I^2C-bus compliance).
		I	**CAP0.0 —** Capture input for Timer 0, channel 0.
P0.3/SDA0/ MAT0.0/EINT1	26[3]	I/O	**P0.3 —** General purpose input/output digital pin (GPIO).
		I/O	**SDA0 —** I^2C0 data input/output. Open-drain output (for I^2C-bus compliance).
		O	**MAT0.0 —** Match output for Timer 0, channel 0.
		I	**EINT1 —** External interrupt 1 input.
P0.4/SCK0/ CAP0.1/AD0.6	27[4]	I/O	**P0.4 —** General purpose input/output digital pin (GPIO).
		I/O	**SCK0 —** Serial clock for SPI0. SPI clock output from master or input to slave.
		I	**CAP0.1 —** Capture input for Timer 0, channel 0.
		I	**AD0.6 —** ADC 0, input 6.
P0.5/MISO0/ MAT0.1/AD0.7	29[4]	I/O	**P0.5 —** General purpose input/output digital pin (GPIO).
		I/O	**MISO0 —** Master In Slave OUT for SPI0. Data input to SPI master or data output from SPI slave.
		O	**MAT0.1 —** Match output for Timer 0, channel 1.
		I	**AD0.7 —** ADC 0, input 7.
P0.6/MOSI0/ CAP0.2/AD1.0	30[4]	I/O	**P0.6 —** General purpose input/output digital pin (GPIO).
		I/O	**MOSI0 —** Master Out Slave In for SPI0. Data output from SPI master or data input to SPI slave.
		I	**CAP0.2 —** Capture input for Timer 0, channel 2.
		I	**AD1.0 —** ADC 1, input 0. Available in LPC2144/46/48 only.
P0.7/SSEL0/ PWM2/EINT2	31[2]	I/O	**P0.7 —** General purpose input/output digital pin (GPIO).
		I	**SSEL0 —** Slave Select for SPI0. Selects the SPI interface as a slave.
		O	**PWM2 —** Pulse Width Modulator output 2.
		I	**EINT2 —** External interrupt 2 input.
P0.8/TXD1/ PWM4/AD1.1	33[4]	I/O	**P0.8 —** General purpose input/output digital pin (GPIO).
		O	**TXD1 —** Transmitter output for UART1.
		O	**PWM4 —** Pulse Width Modulator output 4.
		I	**AD1.1 —** ADC 1, input 1. Available in LPC2144/46/48 only.

Symbol	Pin	Type	Description
P0.9/RXD1/ PWM6/EINT3	34[2]	I/O	**P0.9 —** General purpose input/output digital pin (GPIO).
		I	**RXD1 —** Receiver input for UART1.
		O	**PWM6 —** Pulse Width Modulator output 6.
		I	**EINT3 —** External interrupt 3 input.
P0.10/RTS1/ CAP1.0/AD1.2	35[4]	I/O	**P0.10 —** General purpose input/output digital pin (GPIO).
		O	**RTS1 —** Request to Send output for UART1. LPC2144/46/48 only.
		I	**CAP1.0 —** Capture input for Timer 1, channel 0.
		I	**AD1.2 —** ADC 1, input 2. Available in LPC2144/46/48 only.
P0.11/CTS1/ CAP1.1/SCL1	37[3]	I/O	**P0.11 —** General purpose input/output digital pin (GPIO).
		I	**CTS1 —** Clear to Send input for UART1. Available in LPC2144/46/48 only.
		I	**CAP1.1 —** Capture input for Timer 1, channel 1.
		I/O	**SCL1 —** I^2C1 clock input/output. Open-drain output (for I^2C-bus compliance)
P0.12/DSR1/ MAT1.0/AD1.3	38[4]	I/O	**P0.12 —** General purpose input/output digital pin (GPIO).
		I	**DSR1 —** Data Set Ready input for UART1. Available in LPC2144/46/48 only.
		O	**MAT1.0 —** Match output for Timer 1, channel 0.
		I	**AD1.3 —** ADC input 3. Available in LPC2144/46/48 only.
P0.13/DTR1/ MAT1.1/AD1.4	39[4]	I/O	**P0.13 —** General purpose input/output digital pin (GPIO).
		O	**DTR1 —** Data Terminal Ready output for UART1. LPC2144/46/48 only.
		O	**MAT1.1 —** Match output for Timer 1, channel 1.
		I	**AD1.4 —** ADC input 4. Available in LPC2144/46/48 only.
P0.14/DCD1/ EINT1/SDA1	41[3]	I/O	**P0.14 —** General purpose input/output digital pin (GPIO).
		I	**DCD1 —** Data Carrier Detect input for UART1. LPC2144/46/48 only.
		I	**EINT1 —** External interrupt 1 input.
		I/O	**SDA1 —** I^2C1 data input/output. Open-drain output (for I^2C-bus compliance) **Note:** LOW on this pin while $\overline{\text{RESET}}$ is LOW forces on-chip boot loader to take over control of the part after reset.
P0.15/RI1/ EINT2/AD1.5	45[4]	I/O	**P0.15 —** General purpose input/output digital pin (GPIO).
		I	**RI1 —** Ring Indicator input for UART1. Available in LPC2144/46/48 only.
		I	**EINT2 —** External interrupt 2 input.
		I	**AD1.5 —** ADC 1, input 5. Available in LPC2144/46/48 only.
P0.16/EINT0/ MAT0.2/CAP0.2	46[2]	I/O	**P0.16 —** General purpose input/output digital pin (GPIO).
		I	**EINT0 —** External interrupt 0 input.
		O	**MAT0.2 —** Match output for Timer 0, channel 2.
		I	**CAP0.2 —** Capture input for Timer 0, channel 2.
P0.17/CAP1.2/ SCK1/MAT1.2	47[1]	I/O	**P0.17 —** General purpose input/output digital pin (GPIO).
		I	**CAP1.2 —** Capture input for Timer 1, channel 2.
		I/O	**SCK1 —** Serial Clock for SSP. Clock output from master or input to slave.
		O	**MAT1.2 —** Match output for Timer 1, channel 2.

Symbol	Pin	Type	Description
P0.18/CAP1.3/ MISO1/MAT1.3	53[1]	I/O	**P0.18 —** General purpose input/output digital pin (GPIO).
		I	**CAP1.3 —** Capture input for Timer 1, channel 3.
		I/O	**MISO1 —** Master In Slave Out for SSP. Data input to SPI master or data output from SSP slave.
		O	**MAT1.3 —** Match output for Timer 1, channel 3.
P0.19/MAT1.2/ MOSI1/CAP1.2	54[1]	I/O	**P0.19 —** General purpose input/output digital pin (GPIO).
		O	**MAT1.2 —** Match output for Timer 1, channel 2.
		I/O	**MOSI1 —** Master Out Slave In for SSP. Data output from SSP master or data input to SSP slave.
		I	**CAP1.2 —** Capture input for Timer 1, channel 2.
P0.20/MAT1.3/ SSEL1/EINT3	55[2]	I/O	**P0.20 —** General purpose input/output digital pin (GPIO).
		O	**MAT1.3 —** Match output for Timer 1, channel 3.
		I	**SSEL1 —** Slave Select for SSP. Selects the SSP interface as a slave.
		I	**EINT3 —** External interrupt 3 input.
P0.21/PWM5/ AD1.6/CAP1.3	1[4]	I/O	**P0.21 —** General purpose input/output digital pin (GPIO).
		O	**PWM5 —** Pulse Width Modulator output 5.
		I	**AD1.6 —** ADC 1, input 6. Available in LPC2144/46/48 only.
		I	**CAP1.3 —** Capture input for Timer 1, channel 3.
P0.22/AD1.7/ CAP0.0/MAT0.0	2[4]	I/O	**P0.22 —** General purpose input/output digital pin (GPIO).
		I	**AD1.7 —** ADC 1, input 7. Available in LPC2144/46/48 only.
		I	**CAP0.0 —** Capture input for Timer 0, channel 0.
		O	**MAT0.0 —** Match output for Timer 0, channel 0.
P0.23/V_{BUS}	58[1]	I/O	**P0.23 —** General purpose input/output digital pin (GPIO).
		I	**V_{BUS} —** Indicates the presence of USB bus power. **Note:** This signal must be HIGH for USB reset to occur.
P0.25/AD0.4/ AOUT	9[5]	I/O	**P0.25 —** General purpose input/output digital pin (GPIO).
		I	**AD0.4 —** ADC 0, input 4.
		O	**AOUT —** DAC output. Available in LPC2142/44/46/48 only.
P0.28/AD0.1/ CAP0.2/MAT0.2	13[4]	I/O	**P0.28 —** General purpose input/output digital pin (GPIO).
		I	**AD0.1 —** ADC 0, input 1.
		I	**CAP0.2 —** Capture input for Timer 0, channel 2.
		O	**MAT0.2 —** Match output for Timer 0, channel 2.
P0.29/AD0.2/ CAP0.3/MAT0.3	14[4]	I/O	**P0.29 —** General purpose input/output digital pin (GPIO).
		I	**AD0.2 —** ADC 0, input 2.
		I	**CAP0.3 —** Capture input for Timer 0, Channel 3.
		O	**MAT0.3 —** Match output for Timer 0, channel 3.
P0.30/AD0.3/ EINT3/CAP0.0	15[4]	I/O	**P0.30 —** General purpose input/output digital pin (GPIO).
		I	**AD0.3 —** ADC 0, input 3.
		I	**EINT3 —** External interrupt 3 input.
		I	**CAP0.0 —** Capture input for Timer 0, channel 0.

Symbol	Pin	Type	Description
P0.31/UP_LED/ CONNECT	17[6]	O	**P0.31 —** General purpose output only digital pin (GPO).
		O	**UP_LED —** USB GoodLink LED indicator. It is LOW when device is configured (non-control endpoints enabled). It is HIGH when the device is not configured or during global suspend.
		O	**CONNECT —** Signal used to switch an external 1.5 kΩ resistor under the software control. Used with the SoftConnect USB feature. **Important:** This is an digital output only pin. This pin MUST NOT be externally pulled LOW when $\overline{\text{RESET}}$ pin is LOW or the JTAG port will be disabled.
P1.0 to P1.31		I/O	**Port 1:** Port 1 is a 32-bit bidirectional I/O port with individual direction controls for each bit. The operation of port 1 pins depends upon the pin function selected via the pin connect block. Pins 0 through 15 of port 1 are not available.
P1.16/ TRACEPKT0	16[6]	I/O	**P1.16 —** General purpose input/output digital pin (GPIO).
		O	**TRACEPKT0 —** Trace Packet, bit 0. Standard I/O port with internal pull-up.
P1.17/ TRACEPKT1	12[6]	I/O	**P1.17 —** General purpose input/output digital pin (GPIO).
		O	**TRACEPKT1 —** Trace Packet, bit 1. Standard I/O port with internal pull-up.
P1.18/ TRACEPKT2	8[6]	I/O	**P1.18 —** General purpose input/output digital pin (GPIO).
		O	**TRACEPKT2 —** Trace Packet, bit 2. Standard I/O port with internal pull-up.
P1.19/ TRACEPKT3	4[6]	I/O	**P1.19 —** General purpose input/output digital pin (GPIO).
		O	**TRACEPKT3 —** Trace Packet, bit 3. Standard I/O port with internal pull-up.
P1.20/ TRACESYNC	48[6]	I/O	**P1.20 —** General purpose input/output digital pin (GPIO).
		O	**TRACESYNC —** Trace Synchronization. Standard I/O port with internal pull-up. **Note:** LOW on this pin while $\overline{\text{RESET}}$ is LOW enables pins P1.25:16 to operate as Trace port after reset.
P1.21/ PIPESTAT0	44[6]	I/O	**P1.21 —** General purpose input/output digital pin (GPIO).
		O	**PIPESTAT0 —** Pipeline Status, bit 0. Standard I/O port with internal pull-up.
P1.22/ PIPESTAT1	40[6]	I/O	**P1.22 —** General purpose input/output digital pin (GPIO).
		O	**PIPESTAT1 —** Pipeline Status, bit 1. Standard I/O port with internal pull-up.
P1.23/ PIPESTAT2	36[6]	I/O	**P1.23 —** General purpose input/output digital pin (GPIO).
		O	**PIPESTAT2 —** Pipeline Status, bit 2. Standard I/O port with internal pull-up.
P1.24/ TRACECLK	32[6]	I/O	**P1.24 —** General purpose input/output digital pin (GPIO).
		O	**TRACECLK —** Trace Clock. Standard I/O port with internal pull-up.
P1.25/EXTIN0	28[6]	I/O	**P1.25 —** General purpose input/output digital pin (GPIO).
		I	**EXTIN0 —** External Trigger Input. Standard I/O with internal pull-up.
P1.26/RTCK	24[6]	I/O	**P1.26 —** General purpose input/output digital pin (GPIO).
		I/O	**RTCK —** Returned Test Clock output. Extra signal added to the JTAG port. Assists debugger synchronization when processor frequency varies. Bidirectional pin with internal pull-up. **Note:** LOW on RTCK while $\overline{\text{RESET}}$ is LOW enables pins P1.31:26 to operate as Debug port after reset.
P1.27/TDO	64[6]	I/O	**P1.27 —** General purpose input/output digital pin (GPIO).
		O	**TDO —** Test Data out for JTAG interface.

Symbol	Pin	Type	Description
P1.28/TDI	60[6]	I/O	**P1.28 —** General purpose input/output digital pin (GPIO).
		I	**TDI —** Test Data in for JTAG interface.
P1.29/TCK	56[6]	I/O	**P1.29 —** General purpose input/output digital pin (GPIO).
		I	**TCK —** Test Clock for JTAG interface.
P1.30/TMS	52[6]	I/O	**P1.30 —** General purpose input/output digital pin (GPIO).
		I	**TMS —** Test Mode Select for JTAG interface.
P1.31/$\overline{TRST}$	20[6]	I/O	**P1.31 —** General purpose input/output digital pin (GPIO).
		I	**$\overline{TRST}$ —** Test Reset for JTAG interface.
D+	10[7]	I/O	USB bidirectional D+ line.
D–	11[7]	I/O	USB bidirectional D– line.
$\overline{RESET}$	57[8]	I	**External reset input:** A LOW on this pin resets the device, causing I/O ports and peripherals to take on their default states, and processor execution to begin at address 0. TTL with hysteresis, 5 V tolerant.
XTAL1	62[9]	I	Input to the oscillator circuit and internal clock generator circuits.
XTAL2	61[9]	O	Output from the oscillator amplifier.
RTXC1	3[9]	I	Input to the RTC oscillator circuit.
RTXC2	5[9]	O	Output from the RTC oscillator circuit.
V_{SS}	6, 18, 25, 42, 50	I	**Ground:** 0 V reference.
V_{SSA}	59	I	**Analog ground:** 0 V reference. This should nominally be the same voltage as V_{SS}, but should be isolated to minimize noise and error.
V_{DD}	23, 43, 51	I	**3.3 V power supply:** This is the power supply voltage for the core and I/O ports.
V_{DDA}	7	I	**Analog 3.3 V power supply:** This should be nominally the same voltage as V_{DD} but should be isolated to minimize noise and error. This voltage is only used to power the on-chip ADC(s) and DAC.
VREF	63	I	**ADC reference voltage:** This should be nominally less than or equal to the V_{DD} voltage but should be isolated to minimize noise and error. Level on this pin is used as a reference for ADC(s) and DAC.
VBAT	49	I	**RTC power supply voltage:** 3.3 V on this pin supplies the power to the RTC.

DALLAS SEMICONDUCTOR

DS80C320/DS80C323
High–Speed/Low–Power Micro

General Description:

The DS80C320/DS80C323 is a fast 80C31/80C32– compatible microcontroller. Wasted clock and memory cycles have been removed using a redesigned processor core. As a result, every 8051 instruction is executed between 1.5 and 3 times faster than the original for the same crystal speed. Typical applications will see a speed improvement of 2.5 times using the same code and same crystal. The DS80C320/DS80C323 offers a maximum crystal rate of 33 MHz, resulting in apparent execution speeds of 82.5 MHz (approximately 2.5X).

The DS80C320/DS80C323 is pin compatible with all three packages of the standard 80C32 and offers the same timer/counters, serial port, and I/O ports. In short, the device is extremely familiar to 8051 users but provides the speed of a 16–bit processor. The DS80C320 provides several extras in addition to greater speed. These include a second full hardware serial port, seven additional interrupts, programmable watchdog timer, power–fail interrupt and reset. The device also provides dual data pointers (DPTRs) to speed block data memory moves. It can also adjust the speed of off–chip data memory access to between two and nine machine cycles for flexibility in selecting memory and peripherals.

The DS80C320 operating voltage ranges from 4.25V to 5.5V, making it ideal as a high–performance upgrade to existing 5V systems. For applications in which power consumption is critical, the DS80C323 offers the same feature set as the DS80C320, but with 2.7V to 5.5V operation.

Pin Assignment:

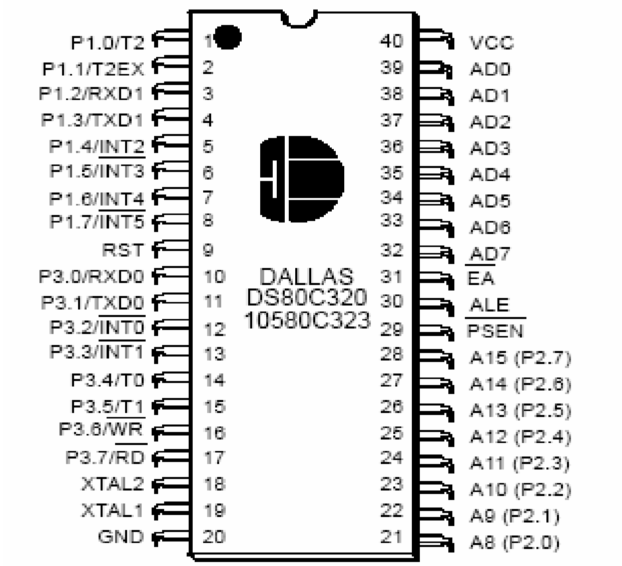

40–PIN DIP

Features:

80C32–Compatible

– 8051 Pin and instruction set compatible
– Four 8–bit I/O ports
– Three 16–bit timer/counters
– 256 bytes scratchpad RAM
– Addresses 64KB ROM and 64KB RAM

High–speed architecture

– 4 clocks/machine cycle (8032=12)
– DC to 33 MHz (DS80C320)
– DC to 18 MHz (DS80C323)
– Single–cycle instruction in 121 ns
– Uses less power for equivalent work
– Dual data pointer
– Optional variable length MOVX to access fast/ slow RAM/peripherals

High integration controller includes:

– Power–fail reset
– Programmable Watchdog timer
– Early–warning power–fail interrupt

Two full–duplex hardware serial ports

13 total interrupt sources with six external

Available in 40–pin DIP, 44–pin PLCC and TQFP

Pin Description:

DIP	PLCC	TQFP	SIGNAL NAME	DESCRIPTION
40	44	38	V_{CC}	**V_{CC} –** +5V.
20	22, 23	16, 17	GND	**GND –** Digital circuit ground.
9	10	4	RST	**RST – Input**. The RST input pin contains a schmitt voltage input to recognize external active high Reset inputs. The pin also employs an internal pull–down resistor to allow for a combination of wired OR external Reset sources. An RC is not required for power–up, as the device provides this function internally.
18 19	20 21	14 15	XTAL2 XTAL1	**XTAL1, XTAL2 –** The crystal oscillator pins XTAL1 and XTAL2 provide support for parallel resonant, AT cut crystals. XTAL1 acts also as an input in the event that an external clock source is used in place of a crystal. XTAL2 serves as the output of the crystal amplifier.
29	32	26	$\overline{PSEN}$	**$\overline{PSEN}$ – Output**. The Program Store Enable output. This signal is commonly connected to external ROM memory as a chip enable. $\overline{PSEN}$ will provide an active low pulse width of 2.25 XTAL1 cycles with a period of four XTAL1 cycles. $\overline{PSEN}$ is driven high when data memory (RAM) is being accessed through the bus and during a reset condition.
30	33	27	ALE	**ALE – Output**. The Address Latch Enable output functions as a clock to latch the external address LSB from the multiplexed address/data bus. This signal is commonly connected to the latch enable of an external 373 family transparent latch. ALE has a pulse width of 1.5 XTAL1 cycles and a period of four XTAL1 cycles. ALE is forced high when the device is in a Reset condition.
39 38 37 36 35 34 33 32	43 42 41 40 39 38 37 36	37 36 35 34 33 32 31 30	AD0 AD1 AD2 AD3 AD4 AD5 AD6 AD7	**AD0–7 (Port 0) – I/O.** Port 0 is the multiplexed address/data bus. During the time when ALE is high, the LSB of a memory address is presented. When ALE falls, the port transitions to a bidirectional data bus. This bus is used to read external ROM and read/write external RAM memory or peripherals. The Port 0 has no true port latch and can not be written directly by software. The reset condition of Port 0 is high. No pull–up resistors are needed.
1–8	2–9	40–44 1–3	P1.0–P1.7	**Port 1 – I/O**. Port 1 functions as both an 8–bit bidirectional I/O port and an alternate functional interface for Timer 2 I/O, new External Interrupts, and new Serial Port 1. The reset condition of Port 1 is with all bits at a logic 1. In this state, a weak pull–up holds the port high. This condition also serves as an input mode, since any external circuit that writes to the port will overcome the weak pull–up. When software writes a 0 to any port pin, the device will activate a strong pull–down that remains on until either a 1 is written or a reset occurs. Writing a 1 after the port has been at 0 will cause a strong transition driver to turn on, followed by a weaker sustaining pull–up. Once the momentary strong driver turns off, the port once again becomes the output high (and input) state. The alternate modes of Port 1 are outlined as follows: **Port Alternate Function**
1	2	40		**P1.0** T2 External I/O for Timer/Counter 2
2	3	41		**P1.1** T2EX Timer/Counter 2 Capture/Reload Trigger
3	4	42		**P1.2** RXD1 Serial Port 1 Input
4	5	43		**P1.3** TXD1 Serial Port 1 Output
5	6	44		**P1.4** $\overline{INT2}$ External Interrupt 2 (Positive Edge Detect)
6	7	1		**P1.5** $\overline{INT3}$ External Interrupt 3 (Negative Edge Detect)
7	8	2		**P1.6** $\overline{INT4}$ External Interrupt 4 (Positive Edge Detect)
8	9	3		**P1.7** $\overline{INT5}$ External Interrupt 5 (Negative Edge Detect)

DIP	PLCC	TQFP	SIGNAL NAME	DESCRIPTION
21 22 23 24 25 26 27 28	24 25 26 27 28 29 30 31	18 19 20 21 22 23 24 25	A8 (P2.0) A9 (P2.1) A10 (P2.2) A11 (P2.3) A12 (P2.4) A13 (P2.5) A14 (P2.6) A15 (P2.7)	**A15–A8 (Port 2) – Output.** Port 2 serves as the MSB for external addressing. P2.7 is A15 and P2.0 is A8. The device will automatically place the MSB of an address on P2 for external ROM and RAM access. Although Port 2 can be accessed like an ordinary I/O port, the value stored on the Port 2 latch will never be seen on the pins (due to memory access). Therefore writing to Port 2, in software is only useful for the instructions MOVX A, @Ri or MOVX @Ri, A. These instructions use the Port 2 internal latch to supply the external address MSB. In this case, the Port 2 latch value will be supplied as the address information.
10–17	11, 13–19	5, 7–13	P3.0–P3.7	**Port 3 – I/O.** Port 3 functions as both an 8–bit bidirectional I/O port and an alternate functional interface for External Interrupts, Serial Port 0, Timer 0 & 1 Inputs, $\overline{RD}$ and $\overline{WR}$ strobes. The reset condition of Port 3 is with all bits at a logic 1. In this state, a weak pull–up holds the port high. This condition also serves as an input mode, since any external circuit that writes to the port will overcome the weak pull–up. When software writes a 0 to any port pin, the device will activate a strong pull–down that remains on until either a 1 is written or a reset occurs. Writing a 1 after the port has been at 0 will cause a strong transition driver to turn on, followed by a weaker sustaining pull–up. Once the momentary strong driver turns off, the port once again becomes both the output high and input state. The alternate modes of Port 3 are outlined below:
				Port **Alternate Mode**
10	11	5		**P3.0** RXD0 Serial Port 0 Input
11	13	7		**P3.1** TXD0 Serial Port 0 Output
12	14	8		**P3.2** $\overline{INT0}$ External Interrupt 0
13	15	9		**P3.3** $\overline{INT1}$ External Interrupt 1
14	16	10		**P3.4** T0 Timer 0 External Input
15	17	11		**P3.5** T1 Timer 1 External Input
16	18	12		**P3.6** $\overline{WR}$ External Data Memory Write Strobe
17	19	13		**P3.7** $\overline{RD}$ External Data Memory Read Strobe
31	35	29	$\overline{EA}$	**$\overline{EA}$ – Input.** This pin must be connected to ground for proper operation.
–	12 34	6 28	NC	**NC – Reserved.** These pins should not be connected. They are reserved for use with future devices in this family.
–	1	39		**NC – Reserved.** These pins are reserved for additional ground pins on future products.

MAXIM MAX 563 DATA SHEETS

+3.3V-Powered, EIA/TIA-562 Dual Transceiver with Receivers Active in Shutdown

General Description:

The MAX563 is a +3.3V-powered EIA/TIA-562 transceiver with two transmitters and two receivers. Because it implements the EIA/TIA-562 standard, the MAX563 communicates with RS-232 transceivers, yet resumes far less power; this makes it ideal for battery-powered, hand-held computers. And, the MAX563 guarantees a 116kbps data rate while maintaining ±3.7V EIA/TIA-562 signal levels, which makes it compatible with pLink™ software. An on-board charge pump converts the +3.3V supply to the ±6.6V needed to produce the EIA/TIA-562 output voltage levels. Four 0.1µF charge-pump capacitors and a bypass capacitor of similar size are the only external components required. When the MAX563's charge pumps and transmitters are shut down to save power, the receivers remain active to continuously monitor signals from external devices (for example, ring indicator from modems). The two receivers' outputs can be enabled and disabled independently of the shutdown function to allow two ports—generally of different types—to be wire-OR connected at the UART.

Features:

© Guaranteed Interoperability with RS-232

© Operates from a Single +3.0V to +3.6V Supply

© 2 Drivers, 2 Receivers

© Receivers Active in Shutdown Mode

© Low-Power Shutdown: 10µA Max

© Small Package—18-Pin Wide SO

© Three-State TTL/CMOS Receiver Outputs

Pin Configuration:

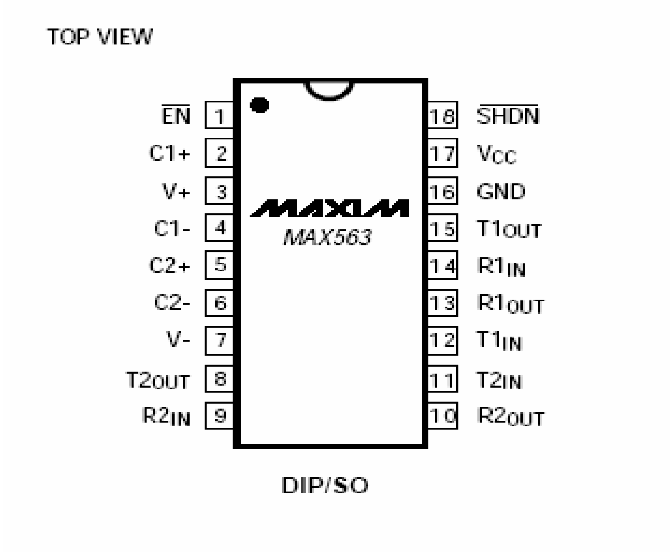

Pin Description:

PIN	NAME	FUNCTION
1	$\overline{EN}$	Receiver enable. Connect $\overline{EN}$ to GND to enable receivers, and take $\overline{EN}$ high to disable receivers.
2	C1+	Positive terminal of positive charge-pump capacitor.
3	V+	+2V_{CC} voltage generated by the positive charge pump. The voltage on V+ collapses to V_{CC} when $\overline{SHDN}$ is low.
4	C1-	Negative terminal of positive charge-pump capacitor.
5	C2+	Positive terminal of inverting charge-pump capacitor.
6	C2-	Negative terminal of inverting charge-pump capacitor.
7	V-	-2V_{CC} voltage generated by the inverting charge pump. The voltage on V- collapses to GND when $\overline{SHDN}$ is low.
8, 15	$T2_{OUT}$, $T1_{OUT}$	EIA/TIA-562 voltage-level transmitter outputs. These outputs are disabled (Hi-Z) when $\overline{SHDN}$ is low.
9, 14	$R2_{IN}$, $R1_{IN}$	EIA/TIA-562 and EIA/TIA-232 voltage-level receiver inputs.
10, 13	$R2_{OUT}$, $R1_{OUT}$	CMOS receiver outputs. These outputs are active regardless of the state of $\overline{SHDN}$. They are enabled when $\overline{EN}$ is low, and disabled (Hi-Z) when $\overline{EN}$ is high.
11, 12	$T2_{IN}$, $T1_{IN}$	CMOS driver inputs.
16	GND	Ground.
17	V_{CC}	+3.0V to +3.6V supply voltage.
18	$\overline{SHDN}$	Shutdown control. Connect to GND to shut down the charge pumps and the transmitters. Take high to turn on the charge pumps and to enable the transmitters.